REPORT DOCUMENTATION PAGE

Form Approved OMB No. 0704-0188

1. AGENCY USE ONLY (Leave blank)	2. REPORT DATE	3. REPORT TYPE AND DATES COVERED
	1995	Final Report

4. TITLE AND SUBTITLE

Analysis of the Near Source and Regional Seismic Records from Mine Explosions in North Caucasus

5. FUNDING NUMBERS

F6170894W0783

6. AUTHOR(S)

Dr. Igor Chernoby

7. PERFORMING ORGANIZATION NAME(S) AND ADDRESS(ES)

Institute of Physics of the Earth
189 Lenin St
Obninsk 249020
Russia

8. PERFORMING ORGANIZATION REPORT NUMBER

N/A

9. SPONSORING/MONITORING AGENCY NAME(S) AND ADDRESS(ES)

EOARD
PSC 802 BOX 14
FPO 09499-0200

10. SPONSORING/MONITORING AGENCY REPORT NUMBER

SPC 94-4088

11. SUPPLEMENTARY NOTES

12a. DISTRIBUTION/AVAILABILITY STATEMENT

Approved for public release; distribution is unlimited.

12b. DISTRIBUTION CODE

A

13. ABSTRACT (Maximum 200 words)

This report results from a contract tasking Institute of Physics of the Earth as follows: Implement a simple portable instrumentation system to document single shot delayed shots at a mine as described in the attached proposal. The data will be used in physical interpretation of regional waveforms.

14. SUBJECT TERMS

EOARD

15. NUMBER OF PAGES

40

16. PRICE CODE

N/A

17. SECURITY CLASSIFICATION OF REPORT	18. SECURITY CLASSIFICATION OF THIS PAGE	19. SECURITY CLASSIFICATION OF ABSTRACT	20. LIMITATION OF ABSTRACT
UNCLASSIFIED	UNCLASSIFIED	UNCLASSIFIED	UL

Technical Report SPC-94-4088

Analysis of the near source and regional seismic records from mine explosions in Northern Caucasus. Discrimination between explosions and regional earthquakes.

Igor Chernobye[1],
Mikhail Zhizhin[2]
Irina Gabsatarova[1]
Dmitry Mechrushev[1]

[1] Russian Academy of Sciences Geophysical Survey, Joint Institute of Physics of the Earth, Obninsk, Russia
[2] Center of Computer Geophysical Data Studies, Joint Institute Physics of the Earth, Moscow, Russia

Russian Academy of Sciences Geophysical Survey, JIPE
189 Lenin St
Obninsk, 249020
Russia
Tel (095) 334-2002

Table of Contents

List of Figures

List of Tables

1. Introduction.

Discrimination between small earthquakes and mine explosions is one of every day problems in regional data processing. Mine explosions often represent a sequence of subexplosions closely grouped in space and time. Baumgardt and Ziegler (1988) found on NORESS array records that such ripple fired events at Scandinavia have modulation of spectra and spectra of earthquakes from the same regions have not. Hedlin *et al.*,(1989) observed similar spectral modulation of quarry blasts records in Kazakhstan and its absence on single-event calibration shots records. In both cases the spectral modulation was observed all over the records from the onset up to Lg coda. This was the basis for the assumption that each subshot in ripple fired one generates the identical wave form and they superpose linearly. Stump and Reinke (1988) have experimentally confirmed validity of these assumptions for small close located explosions. Reamer *et al.*, (1992) on real quarry blasts records have reproduced ripple fired shot convolving single shot record with a set of unit impulses whose time positions correspond to measured delays and include propagation effect. Kim *et al.*, (1994), have found that even in those cases where the observed complex spectral bands do not lead to clear correlation with the spectral bands because of the primary delay times (between the shot holes or between the rows) the spectral scalloping of ripple fired blast records was coherent at stations over wide distance ranges and azimuths. They have also shown that high P/S spectral ratio above 10 Hz is a stable characteristic of instantaneous explosions.

It is evident, that power spectrum modulation may be caused also by near-source geology and propagation path differences. Hedlin *et al.*, (1990) have assumed, that the modulation of a spectrum can be caused by a resonance in low velocity layers near to a source and/or station.

The results on ripple fired shots discriminations have been mainly obtained from high-frequency seismic arrays data analysis. However this problem is also important for the regions, where seismic observations are conducted by networks spread over ~100x100 km area.

In this report the experiment conducted at Tyrnyauz ore mine (Northern Caucasus, Russia) with sophisticated topography is described. This mine produces more than 50% of strongest explosions in the region. The experiment proceeds with field observations that were started in 1993 (Stump *et al.*, 1994). The goals of the experiment -- combination of near-source, local and regional seismic data analysis for the purpose of characterizing important source processes, discrimination between small earthquakes and Tyrnyauz mine explosions recorded by regional seismic network.

During this experiment waveforms generated by well documented close located single, ripple fired near-surface shots and underground ones have been recorded at near-source (200 - 400 m from near-surface shots) distances. Ripple fired and underground shots were also recorded at local (1.5 - 5 km) and regional (25 - 70 km) distances. Single shot records were used for near source ripple fired records modeling. Spectrogram method, P/S spectral ratio and cluster analysis of the wave forms were used to discriminate between mine blasts and regional earthquakes records.

2. Tyrnyauz mine experiment.

The experiment was conducted in October - November 1994 in southern Russia at Tyrnyauz in the Caucasus Mountains. The mine is located in the Kabardino-Balkaria republic, close to the Georgian border. Exploitation has been going on since 1940 in both underground and surface mines between 2000 and 3000 m above see level. More than 150 km of tunnels with diameter of 5.5 m have been dug in the mine. This place is of particular interest for ripple firing effects studies: due to sophisticated topography and ore lode location production shots are carrying out both near surface and 200-700 meters below it in the same vertical plane.

Chemical explosions are usually classified (e.g., Kim *et al.*, 1994) into single, multiple-hole instantaneous and ripple fired ones, depending on the time delays and shooting patterns used. *Multiple-hole instantaneous explosions* are distributed single explosions designed to be detonated within a very short time interval (no more than 8 ms). Following to this classification *ripple fired explosions* most typically consist of 20 - 50 such instantaneous ones with separate delays between them. It was found that some ripple fired explosions have similar characteristics with single shots. These multiple-hole explosions consist of a few rows and/or holes detonated with short delays and are classified as ripple fired explosions with short total duration. For Tyrnyauz mine typical production shots consist of 1 - 5 instantaneous explosions with 20 or 40 ms delay between consecutive detonations. According to the classification above most of explosions in this mine may be classified as instantaneous or ripple fired shots with short total duration.

The waveforms generated by well documented close located single and ripple fired near-surface shots have been recorded at near-source (200-400m), local (1.5-5 km) and regional (25-70 km) distances. Shots and stations locations are shown in Fig. 2.1. The frames in the right and bottom side of the map have the same scale and show more detailed blasts and near-source stations locations for Oct, 16-17 (bottom frame) and Nov, 26-27 (right frame) experiments.

Direct field observations were done to validate on-site shots parameters -- the size and type of borehole, amount and type of explosive, method and timing of detonation. Video film was used to determine the timing and regularity of the explosions.

CM-3KB seismometers with a flat response to velocity between 0.5 and 100 Hz were used for seismic observation at near-source (St1 and St2) and local (PW, BH, LB) stations (Fig. 2.1).

Two 3-component stations (vertical - Z, radial - R, tangential - T) St1 and St2 were installed at 200 and 400 meters distance from nearest borehole. A portable data acquisition system PDAS-100 was used to recover 16-bit data at 500 samples/sec.

Three temporary local stations PW, BH, LB were installed to record mine blasts on Nov, 26-27 at 1.6, 3.4 and 5.6 km distances from near-surface shots. The analog signal was recorded on 2 gain levels (*1,*10) in 0.4 - 20 Hz frequency range. Play-back station recovered 8-bit data for each level at 128 samples/sec.

Timing and location information for each instrument was provided by a GPS receiver.

Stations KNG, KIV, GUM are elements of the regional telemetry network with components provided by Lamont-Doherty Earth Observatory (USA). Recorded signals are 16-bits data in 0.3 - 23 Hz frequency band with sampling rate 60 samples/sec.

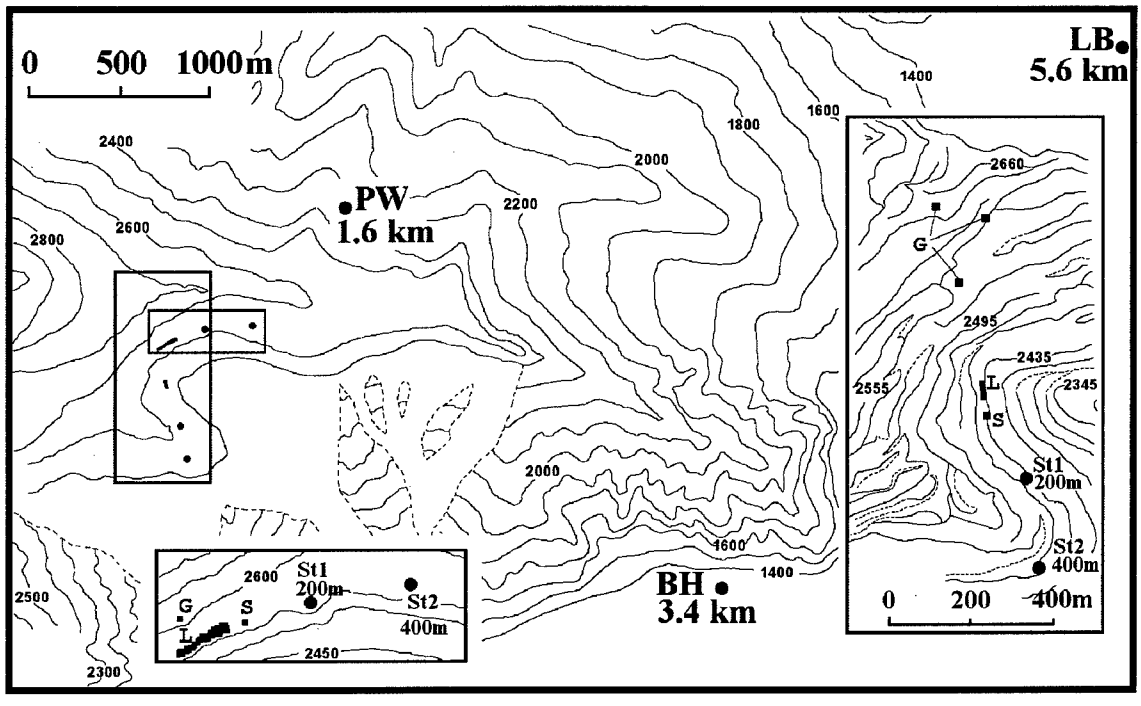

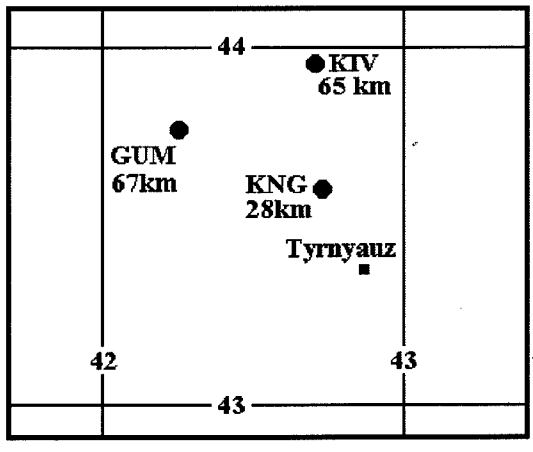

Fig. 2.1 Regional (KIV, GUM, KNG), local (PW, LB, BH) and near-source (St1, St2) stations, mine, underground (G), single (S) and ripple fired (L) near-surface blast locations. In the frames on the right and bottom side of the map - more detailed blasts and near-source stations locations (both frames have the same scale) for Oct, 16-17 (bottom) and Nov, 26-27 (right) experiments.

Two groups of ripple fired and single near-surface shots on Oct, 16-17 and Nov, 26 of 1994 were recorded. The characteristics of the shots are listed in the Table 2.1. Two underground shots were also recorded on Oct, 16 (9.3 tons) and Nov, 27 (24.5 tons).

The locations of the shots are shown in the frames in Fig. 2.1. On Nov, 27 three underground charges shown in the right frame of Fig. 2.1 (from top downwards -- 8.2, 9.8 and 6.5 tons; altitudes 2400, 2255 and 2300 m) were detonated simultaneously. The Oct, 16 underground shot (altitude 2300 m) was detonated 185 m under ripple fired one and in an hour after it. Its location is about 20 m from one of three underground subshots (6.5 tons) detonated on Nov, 27.

Fig. 2.2 (top) shows the ripple fired shots design. The first shot (Oct, 16) consists of 102 boreholes drilled mostly in stripping rocks with decreasing from left to right depth (14 $\rightarrow$ 3 m) and charge (210 $\rightarrow$ 42 kg). The distance between boreholes is 4 - 5 meters. Three rows were detonated with 20 ms time interval. The rest boreholes were detonated simultaneously in 20 ms after third row detonation.

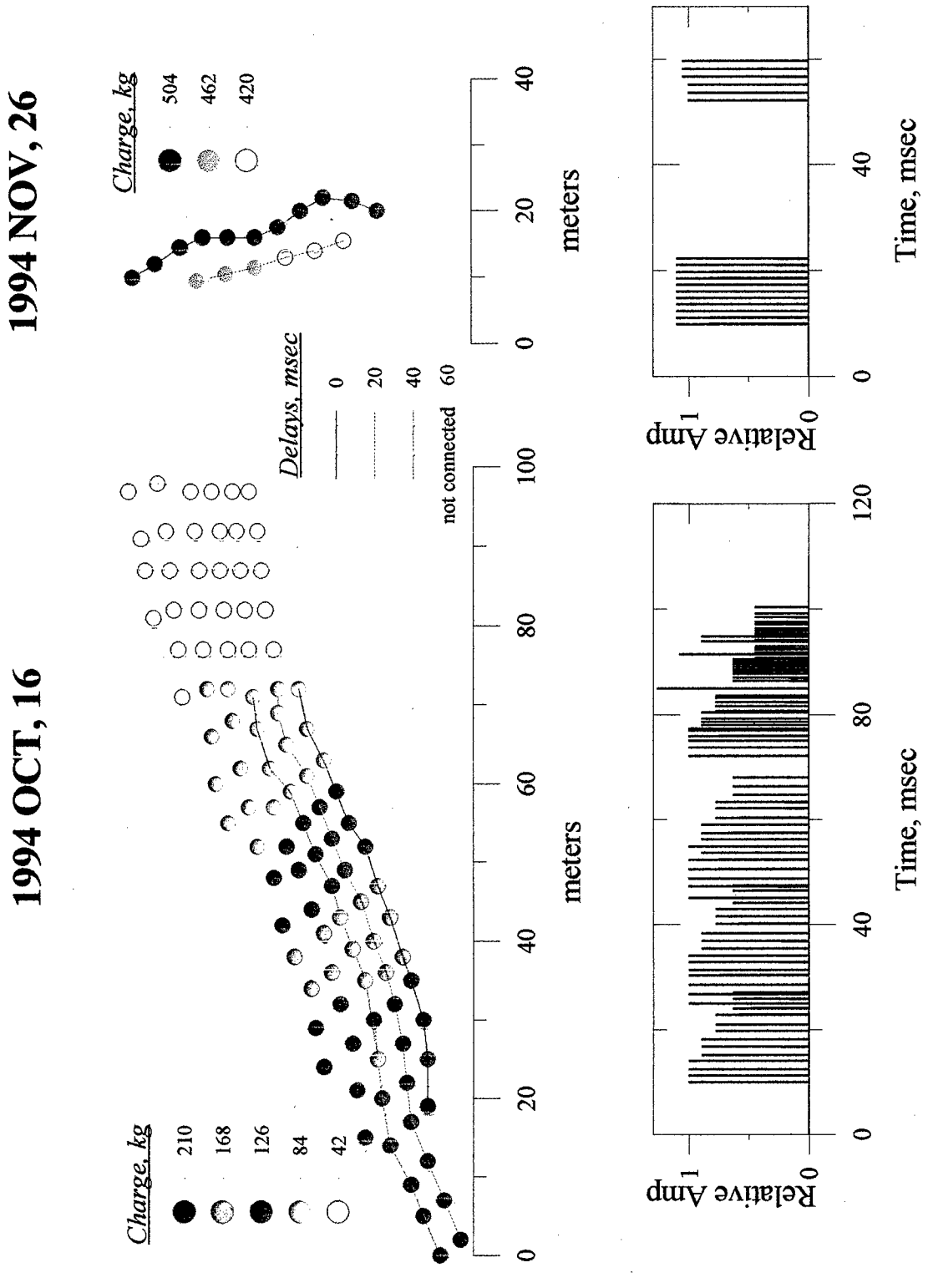

***Fig. 2.2** Ripple fired near-surface shots design. Boreholes are shown by symbols corresponding to the charge value (top). All simultaneously detonated holes (except of ones detonated on Oct, 16 with 60 ms delay) are connected by curves. The sets of the impulses (bottom) that were used for convolution with the single shot records include the delays for traveltimes. The amplitude of individual impulse depends on the charge size.*

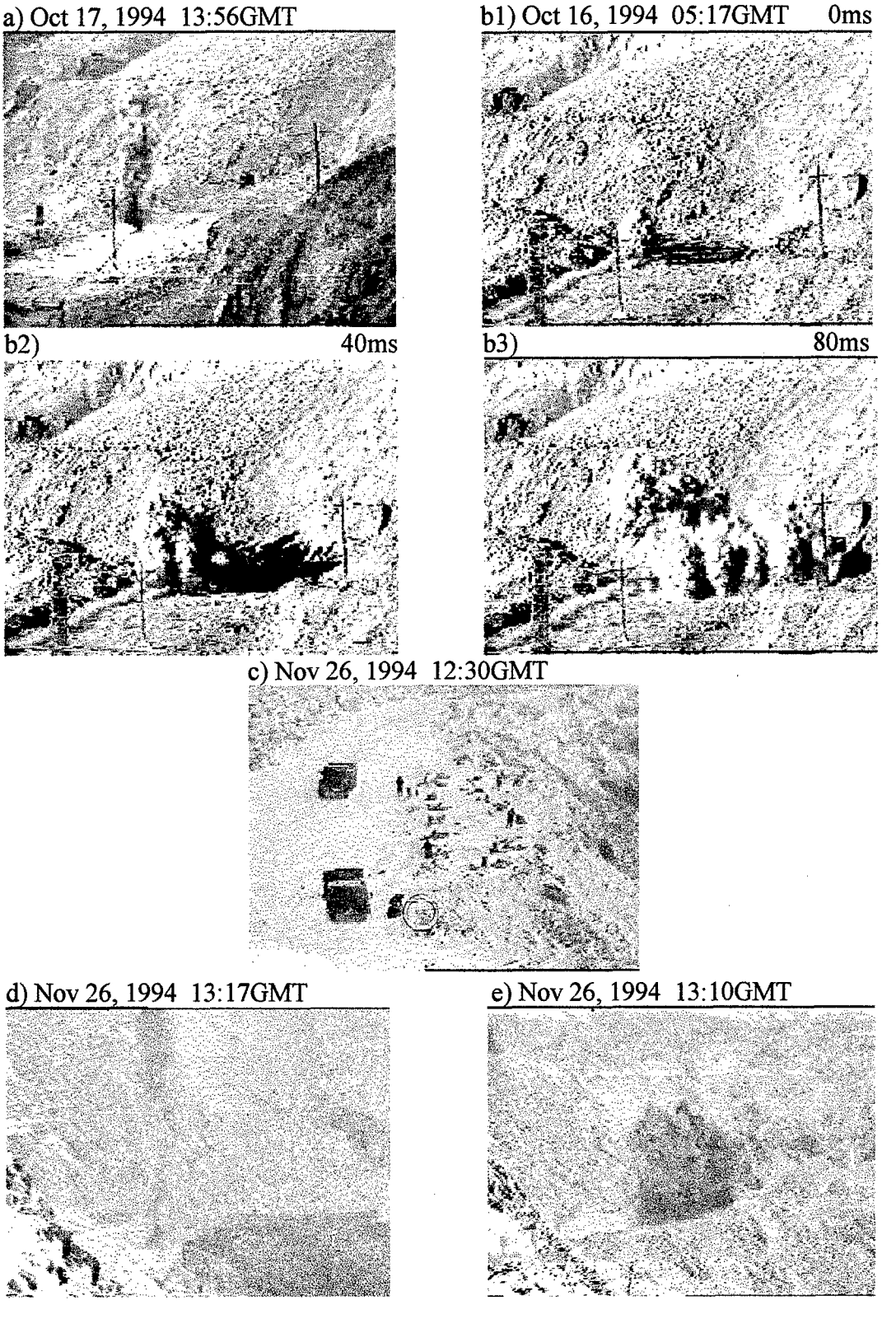

***Fig. 2.3** Video clips of the single and ripple fired explosions. a - Oct, 17 single shot, b1 - b3 -- Oct, 16 ripple fired shot, time interval between frames -- 40 ms; c -- Nov, 26 shots holes locations, single hole is enclosed in red circle; d - single shot, e - ripple fired shot (the first row detonation makes invisible the detonation of the second one).*

The second shot (Nov, 26) consists of 2 rows of 20 m deep boreholes drilled in competent rock. The inner row has 6 charges in line (3 * 420 kg + 3 * 462 kg) separated by 6 meters. The outer row has 11 charges 504 kg each with 5 meters interval. The holes positions follow to the edge of the bank. The outer row (5544 kg) was detonated first, then in 40 ms - the rest 2646 kg. Boreholes are filled with an explosive consisting of granulates (71% of ANN) covered with aluminium powder. The speed of detonation cord is about 7000 m/s. An electrical detonator initiates the firing process with a single pulse. The explosives fragment the rock without concern for mass movement, so the blasts tend to bulk the material moving it primarily in the vertical direction.

Figure 2.3 contains video clips of the single and ripple fired explosions made from St1 side. The single shots were detonated in about 15 meters from the nearest to St1 borehole of each ripple fired shot. The borehole for Nov, 26 single shot was drilled close to the place where bench changes its azimuth on about 30 degrees. Time interval between frames for Oct, 16 shot is 40 ms. The video clips confirm Oct, 16 shot design in Fig. 2.2. Nov, 26 shots occurred in unfavorable for filming whether conditions: snowfall in twilight time (04:10 and 04:17 p.m. local time). All boreholes of the first row were detonated simultaneously and its detonation made invisible the detonation of the second row.

In the bottom of Fig. 2.2 there are two sets of impulses that were used for convolution with the single shot records. The positions of the impulses correspond to delays between rows detonation and include propagation effect.

Table 2.1.

Shot parameters	Single Oct, 17	Ripple fired Oct, 16	Single Nov, 26	Ripple fired Nov, 26
Total charge	210 kg	11970 kg	420 kg	8190 kg
Number of holes	1	102	1	17
Number of rows	-	4	-	2
Depth of the holes	10m	3-14m	20m	20m
Charge per hole	210 kg	42-210 kg	420 kg	420-504 kg
Delay between rows detonation	-	20 ms	-	40 ms
Total duration		60 ms		40 ms
Altitude	2485m	2485m	2435m	2435m

3. Near source data analysis and ripple fired shot records modeling.

The near-source data can be used to evaluate time and frequency domain differences between simultaneous underground and ripple fired, near-surface explosions. To record the waveforms generated by close located both near-surface (single and ripple fired) and underground shots two 3-component (Z, R, T) stations St1 and St2 were installed at the same bench with near-surface shots. Figures 3.1 and 3.2 compare ripple fired, single and underground shots normalized records at St1 and St2 stations obtained on Oct, 16-17 and Nov, 26-27 correspondingly. The coefficients of normalization are shown in the beginning of each trace and are equal to the maximum velocity amplitude (mm/s) of particular record. In October the gain factors at near-source stations were chosen proportional to ones used in previous experiment (Stump *et al.*, 1994) and proved to be too high: most of the data at St1 station are off scale. Single shot on Oct, 17 and tangential component data on Nov, 26-27 were not recorded by St1 due to data acquisition system problems.

The topography around shooting area resulted in remarkable differences between two sets of observations. The St1/St2 ratios of maximum amplitudes records equal to 3 - 5 for Oct, 16 ripple fired shot, and 1.2 - 1.5 for Nov, 26 one. The maximum charge weight per delay is 4660 kg on Oct, 17 and 5540 on Nov, 26. If we consider the same recording distance, blast site and shooting procedure, then according to Nicholls *et al.*, (1971) P waves peak velocities for Nov, 26 records should be about 1.1 of ones for Oct, 16. The ratio observed equals to 1.5 - 5. The ratio of Z component maximum amplitudes, recorded from single near-source shots at St2 stations on Nov, 26 and Oct,27, being equal to 1.35 is close to expected one for charges differ by factor 2 (Table 2.1). The peak amplitudes observed for Oct, 16-17 shots have 1.5 - 3 times bigger values on R-component records in comparison with Z-component ones. The peak amplitudes observed for Nov, 26-27 shots have 1.5 times bigger values on Z-component records from near-surface shots at St1 station. All other but single shot record at St2 station have close peak amplitude values on Z- and R-component. In this case for Nov, 26-27 more complicated propagation paths may be suspected.

Ripple fired shots records in both cases have increased low frequency content relative to single near-surface and underground shots. A significant air blast was introduced on Oct, 16-17 near-surface shot records from multiple shallow holes and/or the lack of stemming in each emplacement hole. These waves have much smaller amplitudes on the records in November because of deeper holes and the fact that instruments were hidden behind jut.

According to Baumgardt and Ziegler (1988) the records of ripple fired or spatially separated events should have time-independent modulation of spectra if signal to noise ratio is big enough within passband of the recording instrument. Such modulation can be represented by frequency-time displays of seismograms, known as sonograms in acoustics (Markel and Gray, 1976). Hedlin *et al.*, (1989; 1990) have implemented an effective method to enhance the time-independent modulation observed on sonogram. Computing spectral estimates for signals recorded at 150 - 250 km distance they have compared for consecutive time windows a relatively

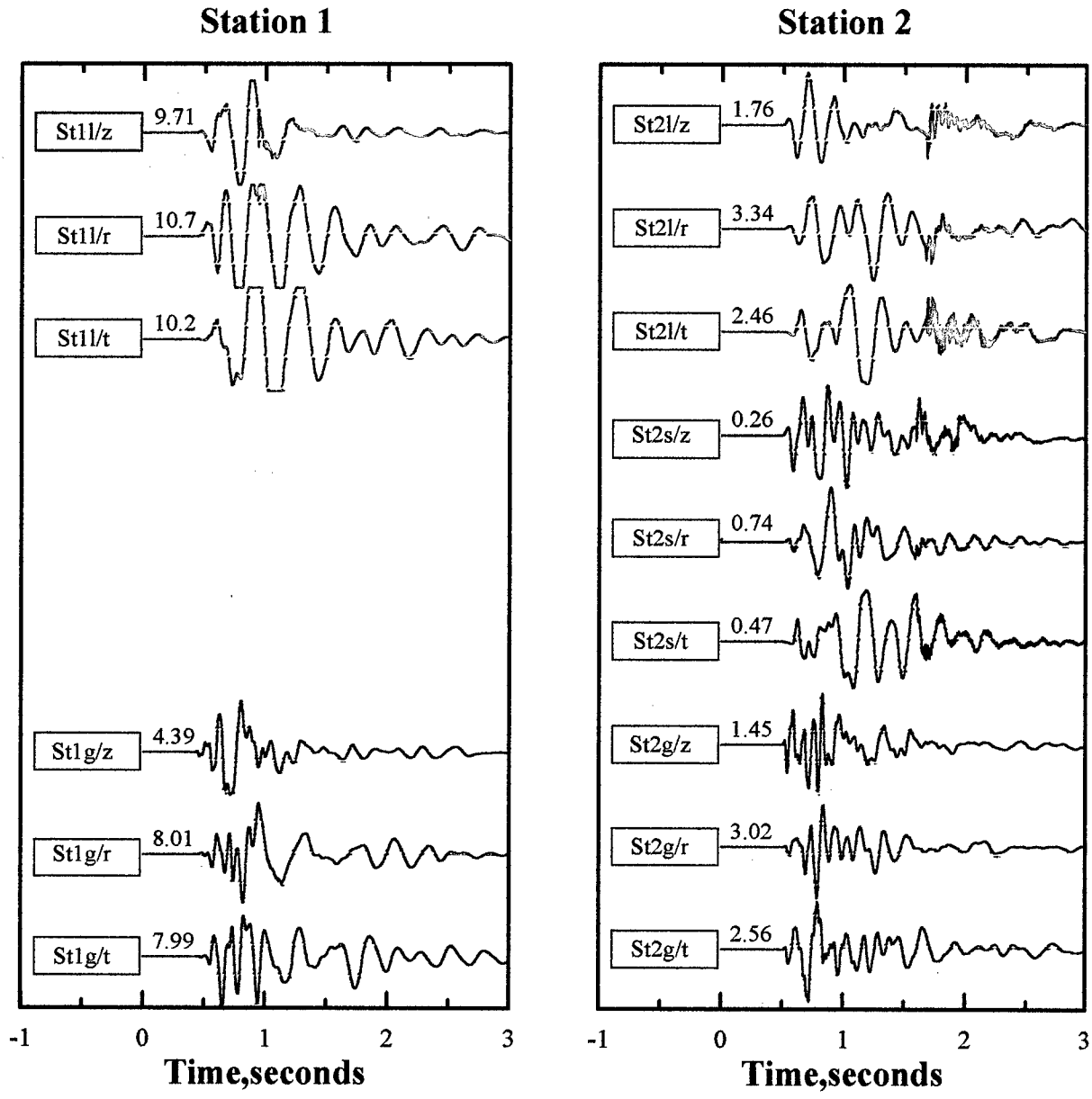

***Fig. 3.1** Oct, 16-17 ripple fired (red), single (blue), and underground (brown) shots normalized records at St1 (left) and St2 (right) stations. The coefficients of normalization are shown in the beginning of each trace and are equal to the maximum velocity amplitude (mm/s) of particular record.*

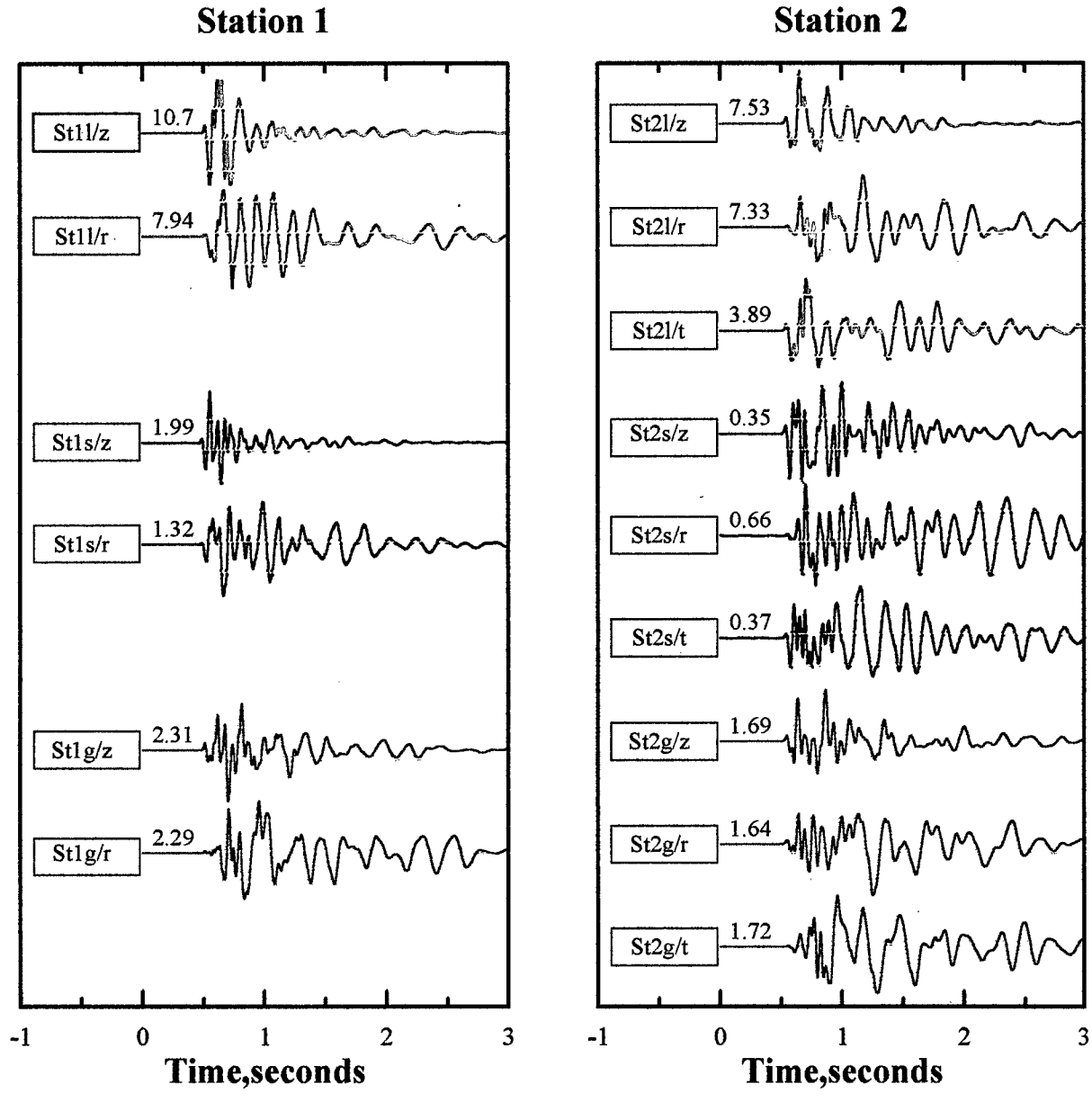

***Fig. 3.2** Nov, 26-27 ripple fired (red), single (blue), and underground (brown) shots normalized records at St1 (left) and St2 (right) stations. The coefficients of normalization are shown in the beginning of each trace and are equal to the maximum velocity amplitude (mm/s) of particular record.*

unsmoothed version of spectral estimate with one that resolves only the large scale structure. In practice, when analyzing these events the smoothed versions were obtained by convolving the original spectral estimates with boxcar functions spanning 2.5 and 1.0 Hz. Than they represent all regions of the sonogram matrix where the local power is high relative to the more regional average power by a value of +1 and where it is low by a -1 getting binary matrix.

In this study demeaned segments of 6 seconds length were selected to calculate spectrograms of near-source records. The segments include about one second of pre-event noise record. Spectral estimates were calculated for 0.512s running window using cosine tapering and 60 ms step (overlapping). To get spectrogram each estimate was convolved with different boxcar functions to resolve time-independent spectral modulation. The resulted spectrograms for ripple fired shots (Oct, 16 and Nov, 26) and spatially separated underground shot (Nov, 27) seismogram recorded at St2 stations (Z component) records are plotted in Fig. 3.3 above corresponding records. Boxcar functions spanning 20 and 4 Hz were used for spectral estimates smoothing. Here local maxima are plotted in black and local minima - in white. The spectrograms of both ripple fired and underground shots seismograms recorded at near-source distances have week modulation during first 300-500 ms only. It may be explained by low spectral resolution achievable at such distances with implemented recording frequency band and/or effects of propagation, near-source topography. Due to St1 and St2 station positions relative first ripple fired shot and short delays the signal from stronger charges crossed the shooting area when closer and weaker charges have been already detonated. In the second case the signal generated by second raw detonation crossed the shooting area of stronger charge.

Particle motion analysis on near-surface and underground shots records has shown that diagrams for single and ripple fired shots are rather similar on some time interval after onset (Fig. 3.4 for October, 16-17 and Fig. 3.5 for November, 26-27 shots): close incidence angle and azimuth, similar frequency content. The diagram for Oct, 16 underground shot is much more complicated. It has higher frequency content and onset's azimuth differs from real direction to the shot. There are a few arrivals within 200 ms time interval after onset caused by multiple reflections between shot and station locations. It should be noted that azimuths of the first arrivals at St2 from Nov, 26 both single and ripple fired shots being identical differ dramatically from the real direction to the source (negative direction of R axis), but the azimuth to the underground shot defined by particle motion analysis fits to the real one. The diagrams for November, 26 near-surface shots show that during the first 200 ms after onset at least 2 wave packages arrive from essentially different angles.

Both local topography and big underground cavities between source and stations suggest an assumption that on Nov, 26 ripple fired shot records may contain echo-signal delayed relative main one. If so, a reflecting surface should exist close (~50 - 150 m) to the shots locations. This echo-signal should also cause modulation of the shots records spectra. Particle motion diagrams of Oct, 16 ripple fired shot records do not prompt the presence of any echo-signal.

The next stage of data analysis is an attempt to reproduce the production ripple fired shots records in time domain by means of frequently used method of linear superpositioning of an observed single shot record with appropriate delay times and amplitudes (Hedlin *et al.*, 1990, Reamer *et al.*, 1992). It is supposed that propagation

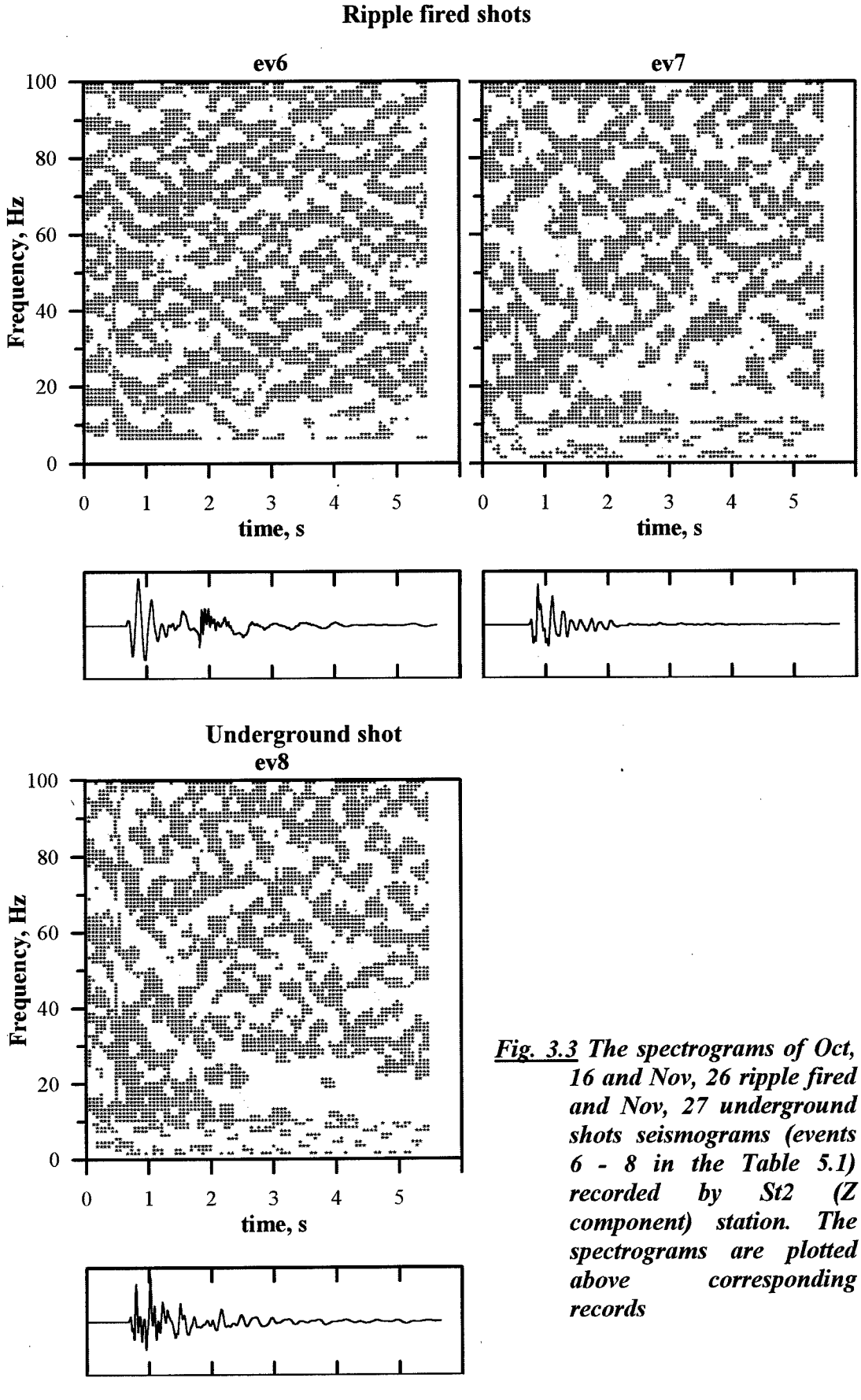

Fig. 3.3 The spectrograms of Oct, 16 and Nov, 26 ripple fired and Nov, 27 underground shots seismograms (events 6 - 8 in the Table 5.1) recorded by St2 (Z component) station. The spectrograms are plotted above corresponding records

Oct,17 single shot

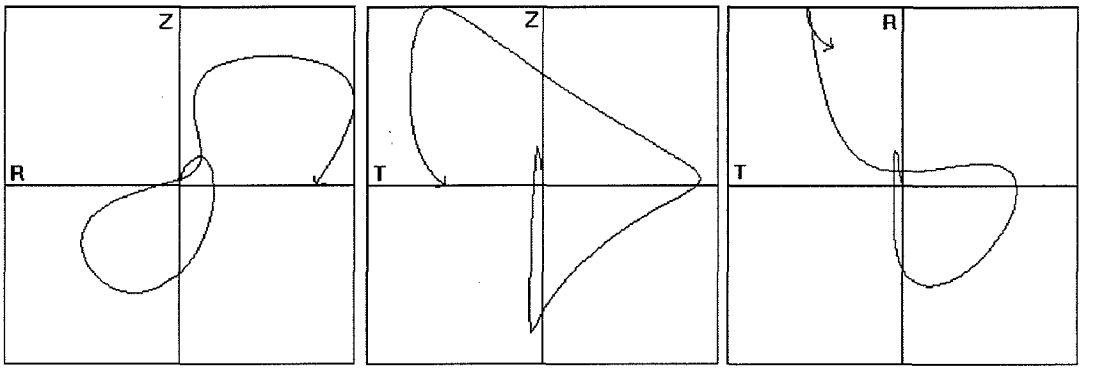

Oct,16 ripple fired shot

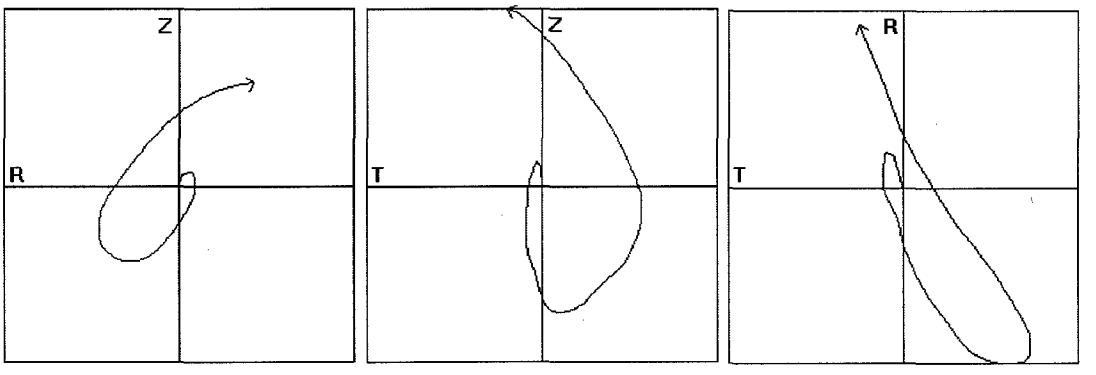

Oct,16 underground shot

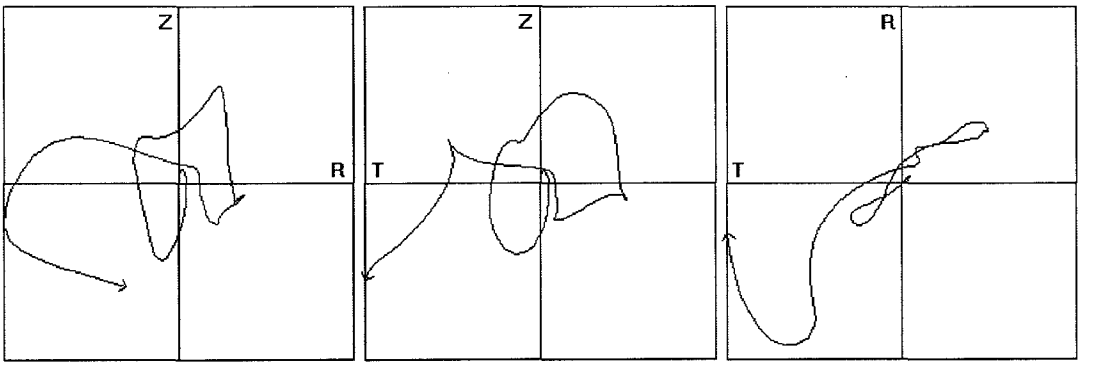

***Fig. 3.4** 200 ms after onset particle motions of Oct, 16-17 ripple fired, single, and underground shots records for St2 station.*

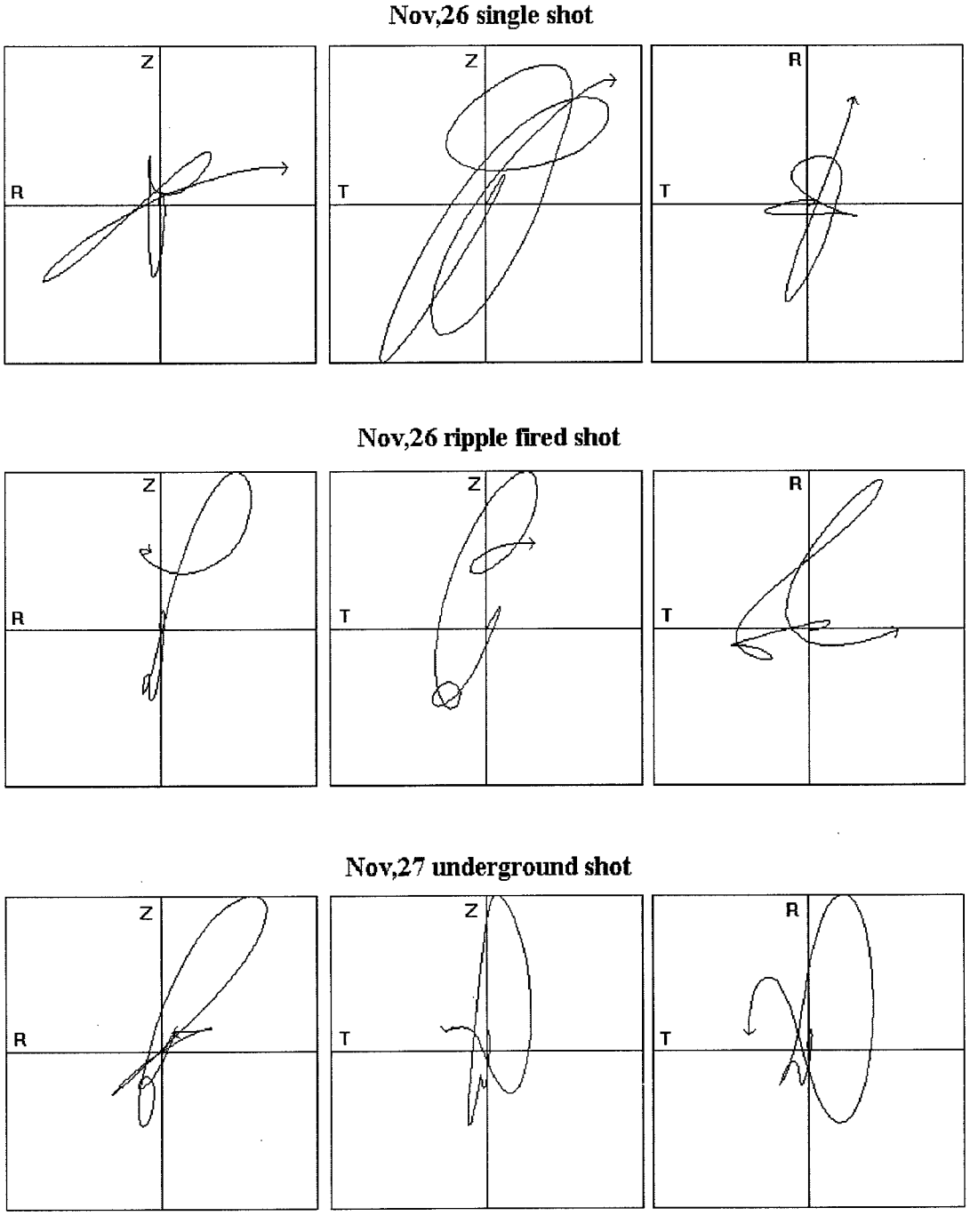

Fig. 3.5 200 ms after onset particle motions of Nov, 26-27 ripple fired, single, and underground shots records for St2 station.

effects and source properties are contained in the recorded signal from a single shot used to synthesize closely located ripple fired shot.

For ripple fired record modeling the near-source data were used only. The single shot records were convolved with a proper set of 102 or 17 impulses (see Fig. 2.2) whose time positions include not only row detonation delay but also assumed compressional wave traveltime. The amplitude assigned to the individual impulse depends on the charge size: it is defined as sqrt of the ratio (subshot charge/single shot charge).

To get synthetic ripple fired shot records it was assumed that the single shot record should already bear the effect of reflection suspected. Occurrence of an additional reflecting surface(s) due to rather big differences in distances between single shot hole and closest and most distant ones of ripple fired shot (15-115 m for Oct, 16 and 15-65m for Nov, 26) was allowed. As far as week modulation is observed at sonograms during first 300-500 ms only the least square method was applied to the first 400 ms of the ripple fired records and synthesized traces. Repeating the convolution of the single shot records with proper modulation function from Fig. 2.2 and such variable parameters as wave propagation velocity along the explosion area Vp (1.5 - 4.5 km/s), delay between rows detonation dt (15 - 25 ms for Oct, 16 and 30 - 50 ms for Nov, 26), echo-signal delay dt1 (if at all) caused by additional reflecting surface (0 - 50 ms), and the ratio of its amplitude to one of initial signal (K = 0 - 1.0) results in a following set of parameters providing the best similarity of synthetic waveform and real record:

for Oct, 16 -- Vp = 3600 m/s, dt = 20 ms, K = 0;
for Nov, 26 -- Vp = 3600 m/s, dt = 40 ms, K = 0.8, dt1 = 30 -32 ms (St1) and K = 0.4 - 0.6, dt1 = 26 ms (St2).

Synthetic records for both ripple fired shots for all components of St2 stations are plotted in Fig. 3.6 together with original records. For Nov, 26 ripple fired shot modeling parameters K = 0.6 and dt1 = 26 ms were used. Synthetic records for Oct, 16 ripple fired shot have 6 - 12 times higher amplitudes than real ones. Nevertheless there is some similarity between real and synthetic records during first 300 - 500 ms after onset. In Fig. 3.7 smoothed (4 Hz window) power spectra of Z, R, T-component St2 records are plotted with power spectra of corresponding set of the impulses from Fig. 2.2 (for Nov, 26 parameters K and dt1 were taken into account). The spectrum of Oct, 16 ripple fired shot record differs significantly from one of the synthetic record. It seems to be caused mainly by poor representation of week and shallow subshots by 2-5 times stronger calibration one: deeper borehole of calibration shot crosses stripping rock layer and is partially buried in competent rock. Stripping rock layer explains also lower high frequency content on Oct, 16 ripple fired shot spectra in comparison with ones for Nov, 26 shot. The comparison of Nov, 26 ripple fired shot and synthetic records spectra shows that they are rather similar in 10-25 Hz frequency band, and positions of the extremums in the spectra fit well enough to ones of the modulation function spectrum up to 80 Hz. The spectrum of the Nov, 26 underground explosion is not more modulated than one of the single Oct, 16 underground shot. As it was shown by particle motion analysis it may be explained by multiple reflections of the waves between source and stations. The October, 16 underground shot records spectra have significantly bigger high frequency content than spectra of stronger both ripple fired shot occurred in an hour 185 m above, and separated in space Nov, 26 underground shot.

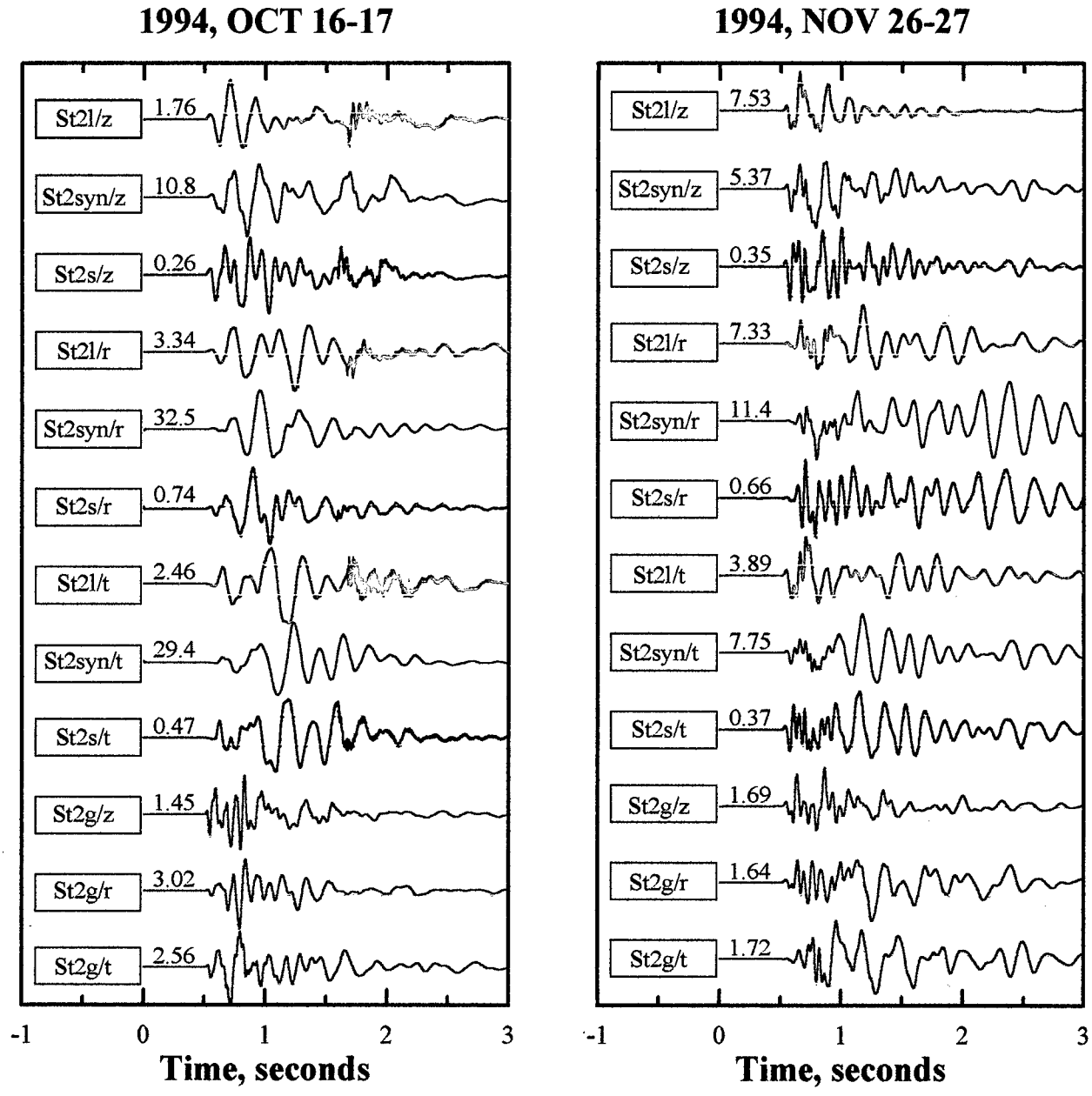

***Fig. 3.6** Ripple fired (l), single (s), and underground (g) shots normalized records at St2 stations on Oct, 16-17 (left) and Nov, 26-27 (right); synthesized (syn) traces of ripple fired shots The coefficients of normalization are shown in the beginning of each trace and are equal to the maximum velocity amplitude (mm/s) of particular record.*

Because of essential topography influence on travel paths it is hard to expect here, that received synthetic seismogram would be similar to the real record all over its length. Comparison of synthetic and ripple fired shot records shows that in this mine where the shift of the source on a few tens of meters effects strongly on wave propagation conditions the envelope similarity can be achieved on the intervals up to 0.3 - 0.5s after onset only (about up to 20% of the records duration).

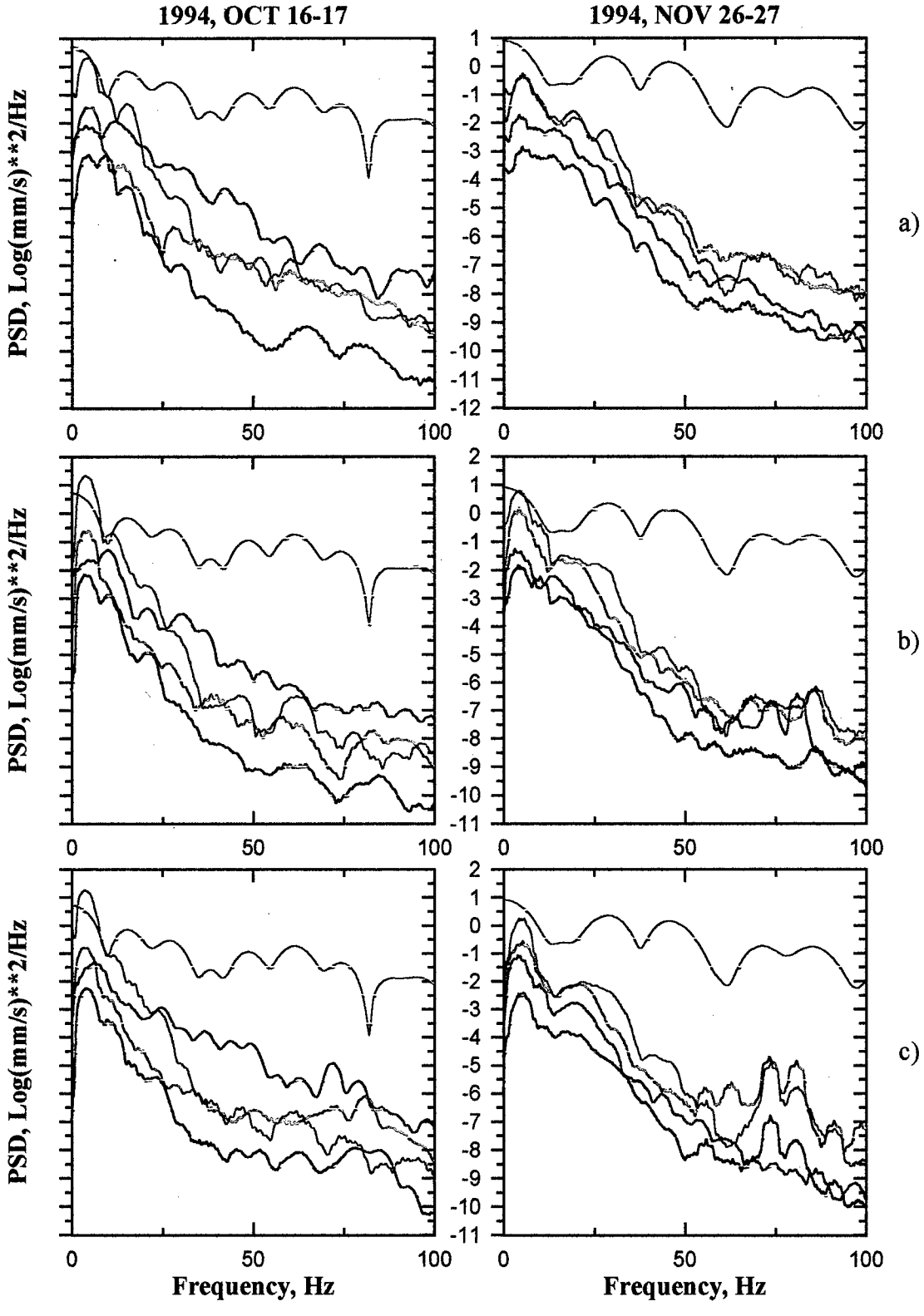

Fig. 3.7 Smoothed (4 Hz window) power spectra of Z(a), R(b), T(c) component records of single (blue), ripple fired (red), underground (brown) shots and synthesized traces (green) from Fig. 3.6. Corresponding modulation functions spectra (upper traces in the frames).

4. Local data analysis

Three temporary local stations PW, BH, LB have been installed to record mine blasts on November, 26-27. The effects of the spatial finiteness of the source begin to decrease at the distances exceeding 2-3 source dimensions (Reamer *et al.*, 1992). Thus, for these stations data analysis Nov, 26 ripple fired shot can be considered as a sequence of two shots whose charges are equal to simultaneously detonated ones and time interval between them equals to delay between rows detonation. If the influence of near source reflecting surface is still observed this pair of impulses will have an echo-signal whose amplitude depends on the coefficient of reflection, and delay - on the relative (source -- *reflecting surface* -- station) position. For stations with different epicentral distances and azimuths different coefficients of reflection and delays are expected. On the other hand the near-source factors providing resonance-type effects at different stations with higher probability will influence at the same frequency band.

The ripple fired and underground shots normalized records at local stations, Z-component whole record power spectra are compared in Fig. 4.1. The coefficients of normalization are shown in the beginning of each trace and are equal to the maximum velocity amplitude (micron per second) of particular record. Underground shot record at PW station was not obtained. On the upper right the spectra of modulating functions corresponding to the case of no echo-signals, as well as to ones delayed on 26, 32 and 36 ms are plotted. As far as the coefficient of reflection being changed between 0.75 and 1 alters local minimum depth and does not shift its position for display purposes the modulation function for K = 0.9 is used. The decay of power spectral density at high frequencies (>20 Hz) is due to the instrument response. The spectral modulation of the ripple fired shot spectra suggests that PW and BH records contain echo-signal with 32 (PW) and 36 (BH) ms delay. It seems there is no echo-signal at LB or this delay is close to 40 ms. The underground shot spectra also have modulation that is caused by spatial distribution:

Demeaned segments of 13 seconds length were selected to calculate spectrograms of BH and LB stations records. The segments include about 3 seconds of pre-event noise record. For PW record the segment has 6 seconds with 1 second of pre-event noise. Spectral estimates were calculated for 1 second of data in running window using cosine tapering and 160 ms step (overlapping). To get spectrogram each spectral estimate was convolved with different boxcar functions to resolve time-independent spectral modulation. The resulted spectrograms for ripple fired (Nov, 26) and spatially separated underground shot (Nov, 27) Z-component seismograms are plotted in figures 4.2 and 4.3 above corresponding records. Boxcar functions spanning 15 and 2 Hz were used for spectral estimates smoothing. For all stations the spectrograms of ripple fired shot have minimum in 14 - 16 Hz frequency range. This minimum becomes not so prominent in a second after onset for PW, and in 2 - 3 seconds for BH and LB records. Its position corresponds to the only minimum of the modulation function (Fig. 4.1) in the instrument passband (0.4 - 20 Hz). The spectrograms of underground shot have similar minima at BH and LB stations. Two of them (around 12 and 16 Hz) are rather stable along the records. Three subshots of underground explosions occurred 150 - 250 m from each other. For shots separated by such distances delays between signals from different subshots will be close to delays between rows detonation for Nov, 26 ripple fired shot and can cause the observed spectral modulation.

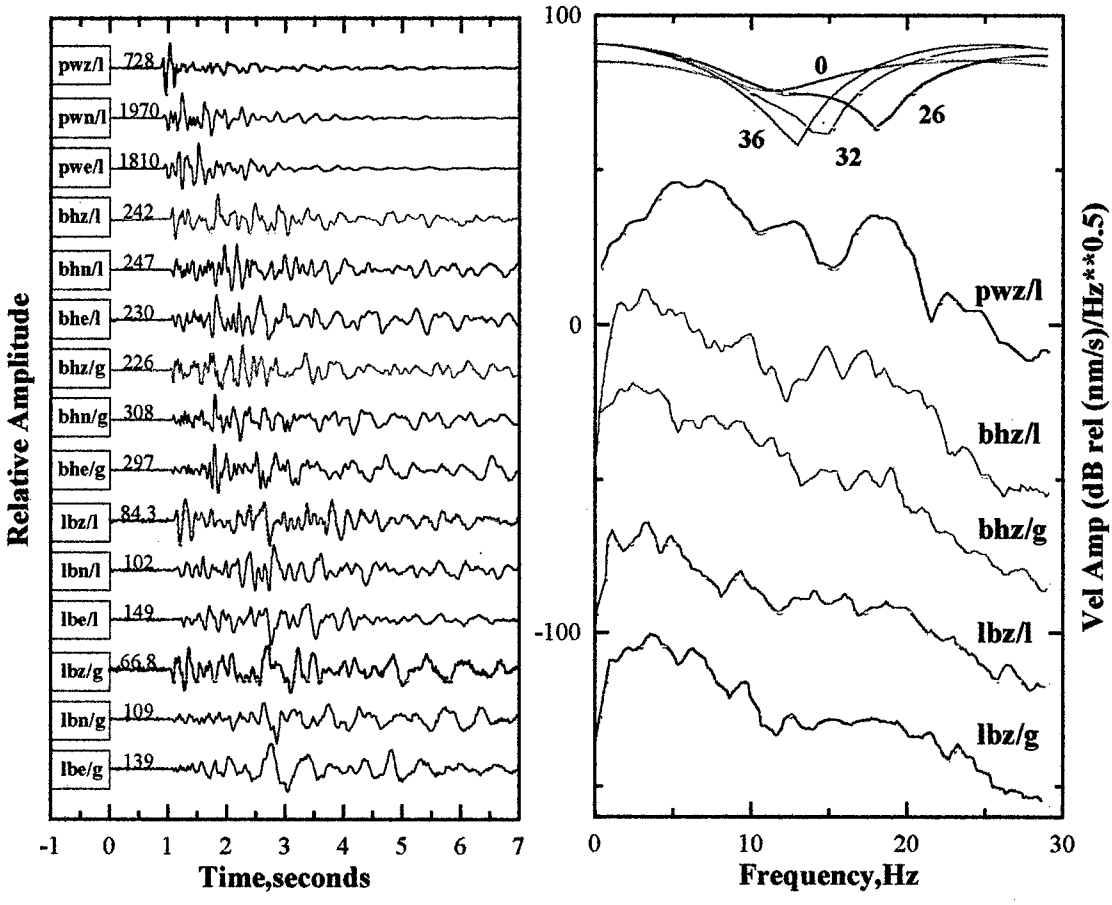

Fig. 4.1 *Comparison of the 3-component (z, n, e) 1994 Nov, 26 ripple-fired (l) and Nov, 27 underground shots (g) records at the stations PW, BH, LB. Spectra of z-component records and modulation functions (upper traces in the right diagram) for the cases of no echo signal (0) due to supposed reflection and ones with echo signal delayed on 26, 32 and 36 sec. Each plot for different records spectra has been shifted by 20 dB for display purposes.*

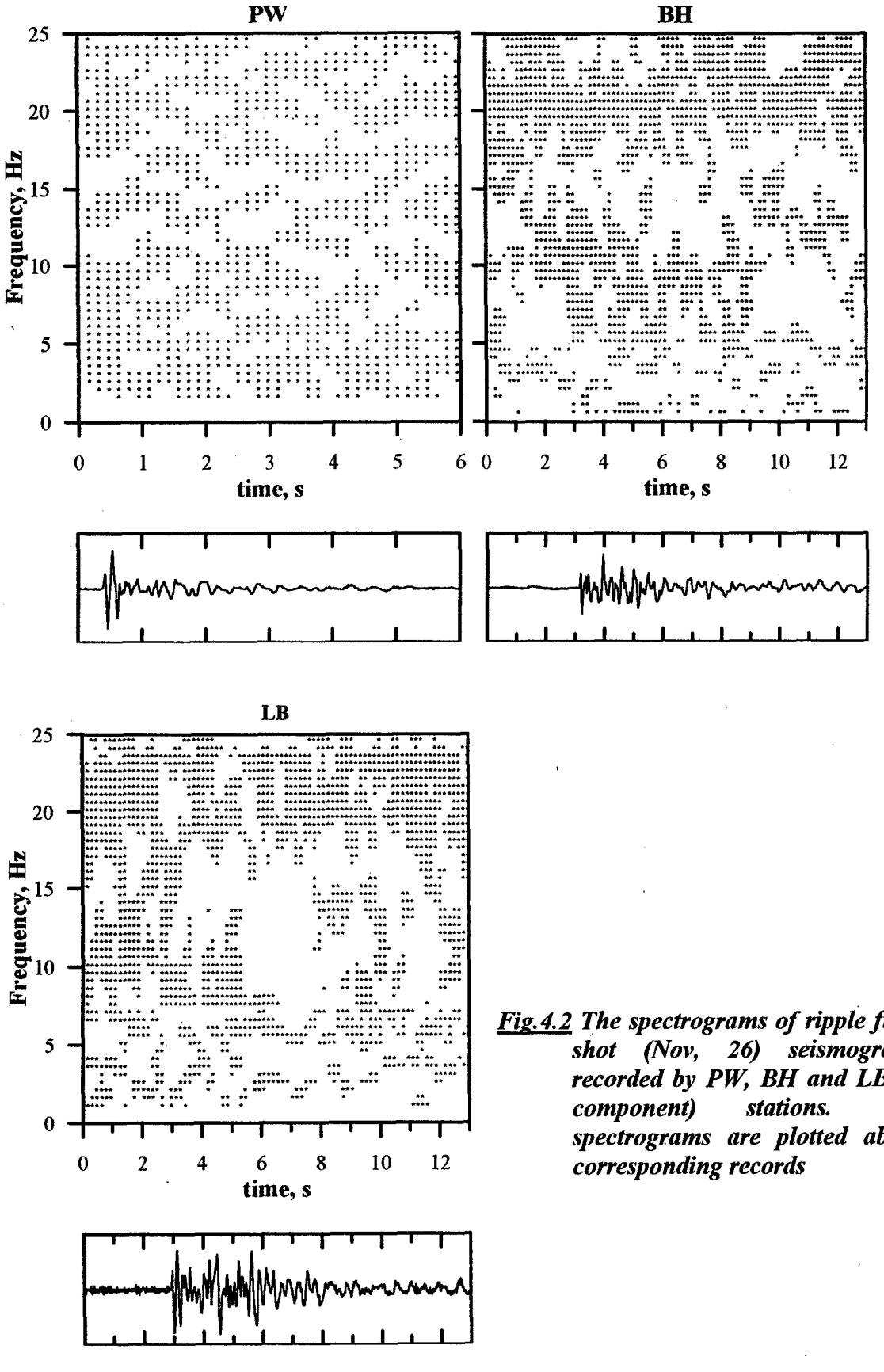

Fig.4.2 The spectrograms of ripple fired shot (Nov, 26) seismograms recorded by PW, BH and LB (Z component) stations. The spectrograms are plotted above corresponding records

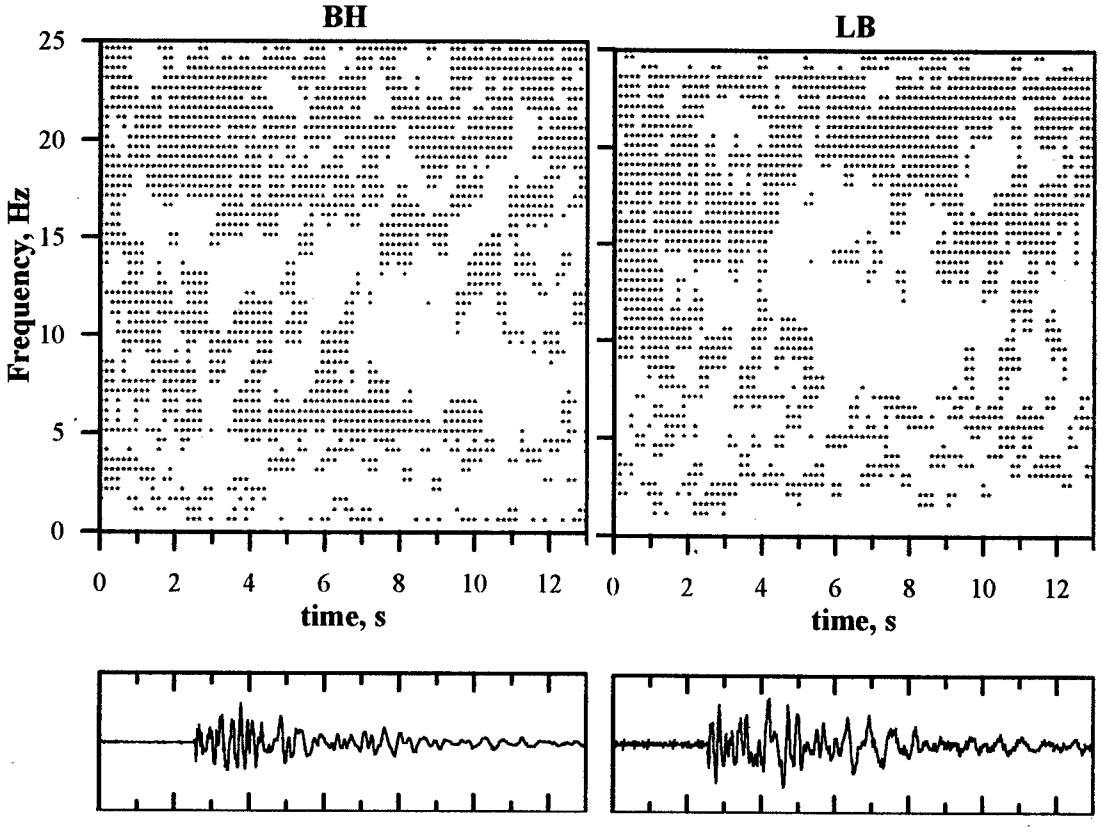

Fig.4.3 The spectrograms of spatially separated underground shot (Nov, 27) seismograms recorded by BH and LB (Z component) stations. The spectrograms are plotted above corresponding records.

The Z-component records of ripple fired shot have clear positive onset at all local stations (Fig. 4.2). The underground shot record at BH(Z) has weak positive onset following by strong negative pulse (Fig. 4.3). At LB(z) one can see strong negative pulse only: the expected positive onset is below noise level. It may be caused by strong attenuation of the waves spreading through worked out area in the mine. In this case P wave reflected from free surface could have stronger amplitude.

5. Regional data analysis. Discrimination between earthquakes and mine blasts

The seismic observations are carried out in Northern Caucasus by regional telemetric systems more than 10 years. There are a few mines in this area that are being operated by different departments. The most often and strongest quarry blasts take place in Tyrnyauz mine in the Kabardino-Balkaria republic, close to the Georgian border. In this study data obtained during experiments in 1993 (Stump *et al.*, 1994) and 1994 (current report) were compared with seismograms of 12 regional earthquakes recorded at regional stations GUM, KIV and KNG (Fig. 2.1). The events are listed in Table 5.1. Ripple fired shots of 1993 have longer total duration - 200 ms (event 2, 25.3 tons) and 120 ms (event 3, 7.3 tons) - than ones of 1994 (see Table 2.1). The Table 5.1 contains data about epicentral distances and azimuths for each station, P wave magnitudes from regional catalog and P/S spectral amplitudes ratios obtained. Spectral and cluster analysis of the waveforms was implemented to discriminate between mine blasts and regional earthquakes records.

Table 5.1

Event N	Data yyddd	Time (utc) hh:mm	Distance km			Azimuth degree			Event type	Magnitude MPSP	P/S		
			KIV	GUM	KNG	KIV	GUM	KNG			KIV	GUM	KNG
1	93234	05:09	65	67	28	167	130	158	g/2	2.8	2.4	2.5	1.9
2	93234	06:24	65	67	28	167	130	158	l/7	3.8	2.5	1.9	1.6
3	93241	05:23	65	67	28	167	130	158	l/4	3.3	2.7	1.7	2.0
4	93241	06:18	65	67	28	167	130	158	g/1	3.0	2.5	1.5*	1.0*
5	94269	06:17	65	67	28	167	130	158	g/1	3.8	2.3	3.7	-
6	94289	05:17	65	67	28	167	130	158	l/4	3.9	3.1	2.2	2.1
7	94330	13:10	65	67	28	167	130	158	l/2	3.8	2.2	2.1	1.9
8	94331	05:39	65	67	28	167	130	158	g/3	3.7	1.8	2.1	1.2
9	94027	16:04	23	64	48	69	63	21	e	4.7	0.8	0.9	0.9
10	94027	16:10	23	64	48	69	63	21	e	4.3	0.8	1.0	0.8
11	94027	16:19	23	64	48	69	63	21	e	2.8	0.8	0.9	0.8
12	94047	13:11	38	80	57	79	70	38	e	4.5	0.9	0.9	-
13	94121	20:44	110	75	84	214	199	230	e	4.7	1.0	0.9	-
14	94127	17:21	110	75	84	214	199	230	e	4.7	1.0	0.9	-
15	94221	04:18	48	61	83	327	09	339	e?	2.8	0.8	0.9	-
16	94287	17:12	26	51	63	335	30	347	e	4.2	0.9	1.0	-
17	94291	21:18	26	51	63	335	30	347	e	4.0	0.8	1.1	-
18	94292	03:06	26	51	63	335	30	347	e	2.8	0.8	0.9	-
19	94042	17:40	211	215	176	151	139	146	e	5.1	0.9	0.6	-
20	94346	13:14	167	173	133	149	135	142	e	5.1	0.6	0.5	-

- Types of events: g - underground shot, l - ripple fired shot, e - earthquake
- /n - for g - number of spatially separated charges,
- for l - number of detonation delays.
- ? - questionable type of event.
- * - low signal/noise ratio

Ripple fired and underground shots Z - component seismograms recorded at KIV, GUM and KNG stations are shown correspondingly in figures 5.1, 5.3, 5.5 with whole records and P, S phases spectra. The whole record spectral estimates were computed from 30 s of data. P and S phase spectra -- from 4 s of data. 20% *cosine* tapering was applied to wave segments. We use here *P phase* without further classification to denote

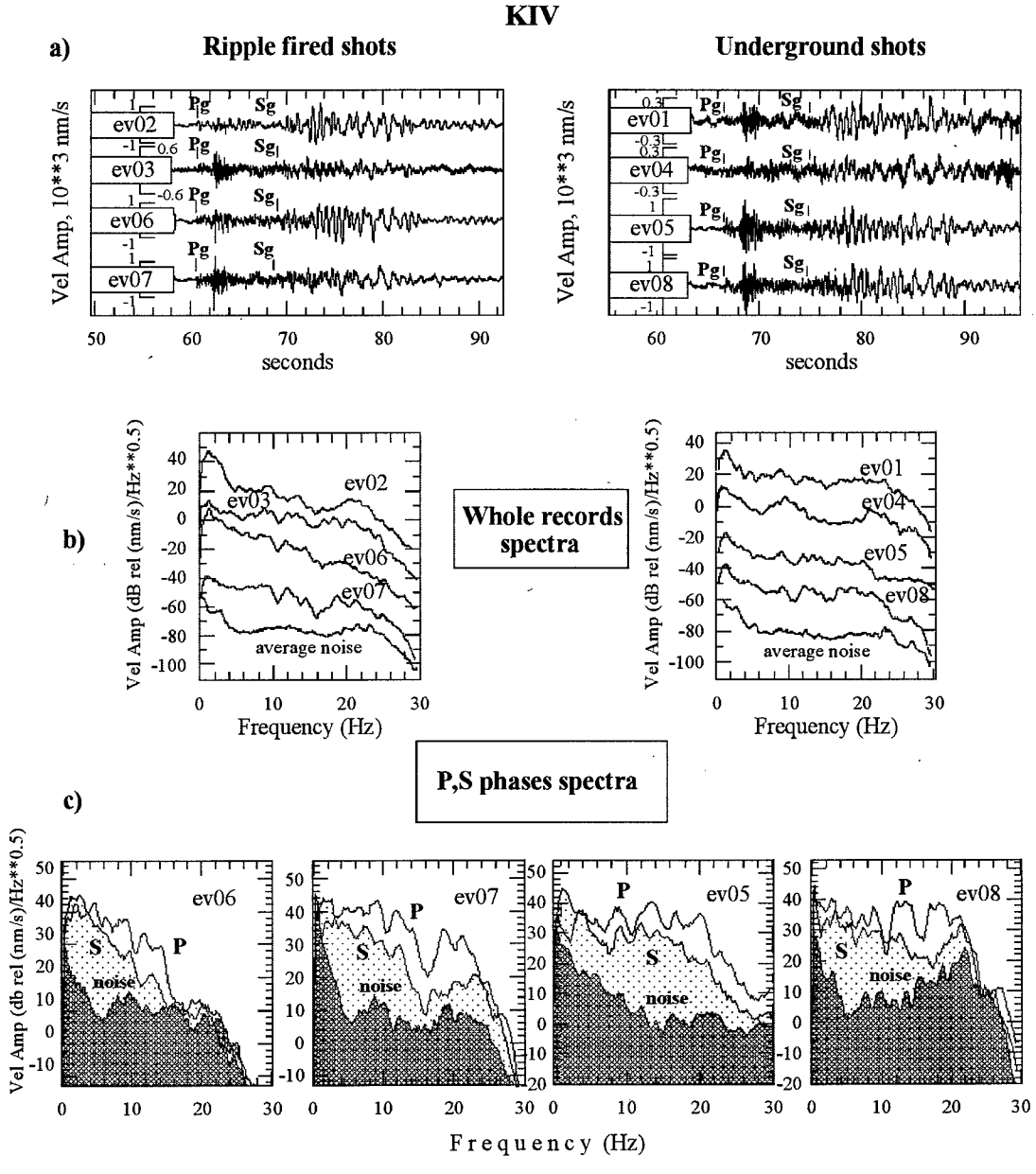

Fig. 5.1 *a - Comparison of Z-component records of ripple fired (l) and underground (g) shots at regional station KIV (Table 5.1, events 1 - 8); b - corresponding whole records spectra. For display purposes Z-component spectra of events and average noise are shifted relative upper trace by correspondingly 20, 60, 80, 80 dB; c - P and S phase spectra.*

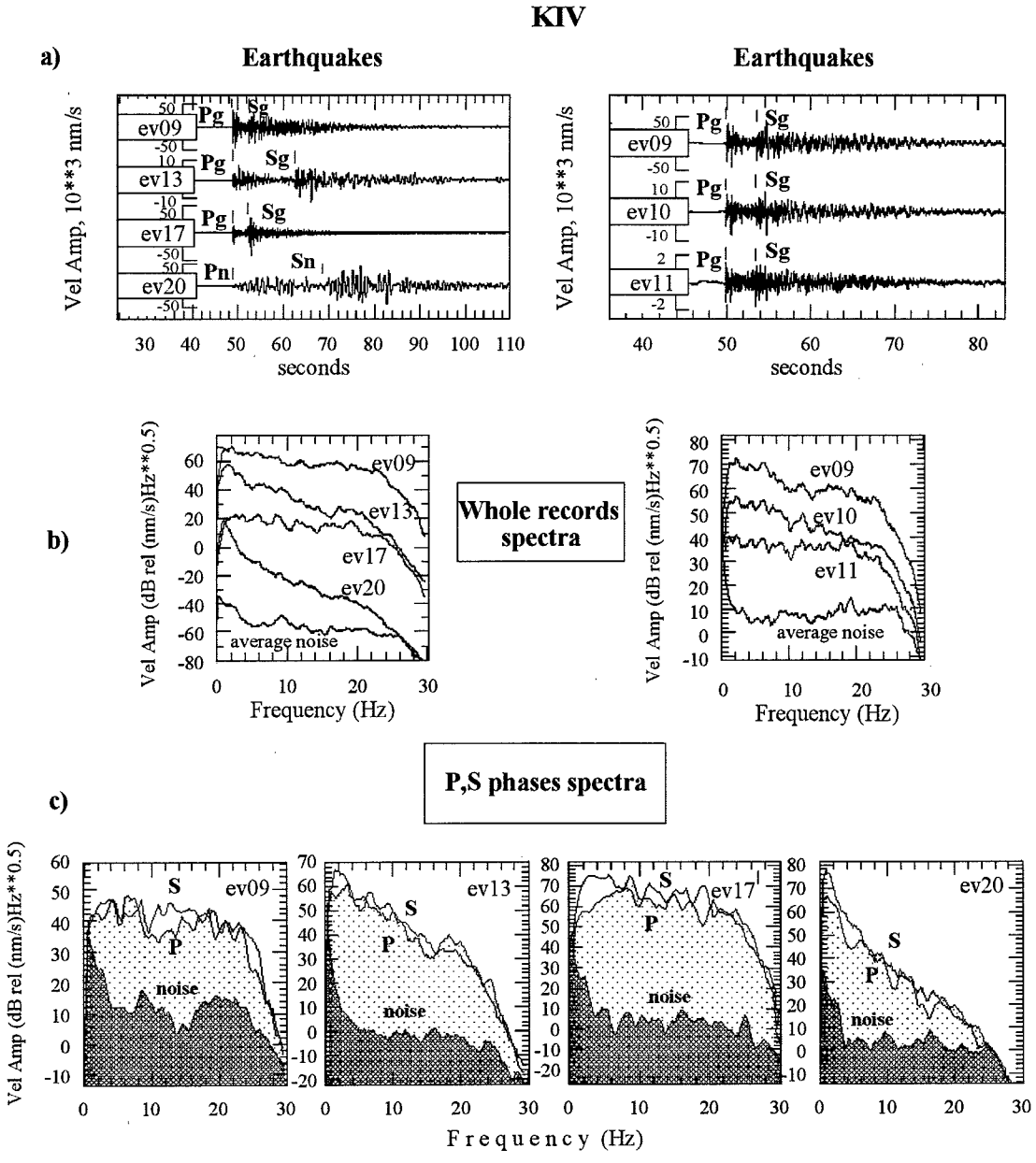

***Fig. 5.2** a - Comparison of Z-component records of regional earthquakes at KIV station (Table 5.1, events 9, 13, 17, 20 - left frame, and events 9, 10, 11 - right frame); b - corresponding whole records spectra. For display purposes Z-component spectra of events 13, 17, 20 and average noise are shifted relative upper trace by correspondingly 12, 40, 60, 60 dB; c - P and S phase spectra.*

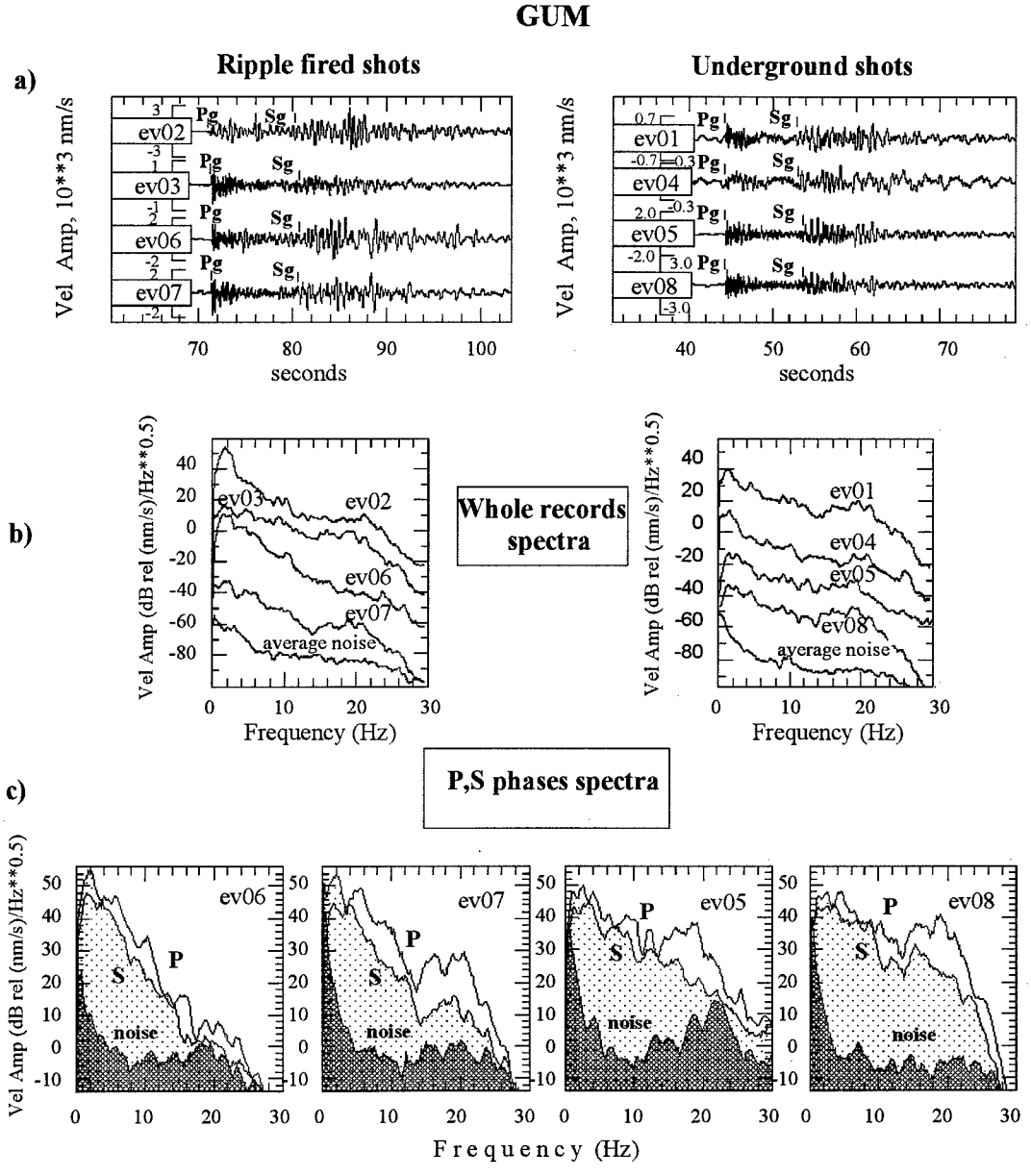

Fig. 5.3 *a - Comparison of Z-component records of ripple fired (l) and underground (g) shots at regional station GUM (Table 5.1, events 1 - 8); b - corresponding whole records spectra. For display purposes Z-component spectra are shifted relative upper trace by correspondingly 20, 40, 80, 80 dB (left frame) and 20, 60, 80, 80 dB (right frame); c - P and S phase spectra.*

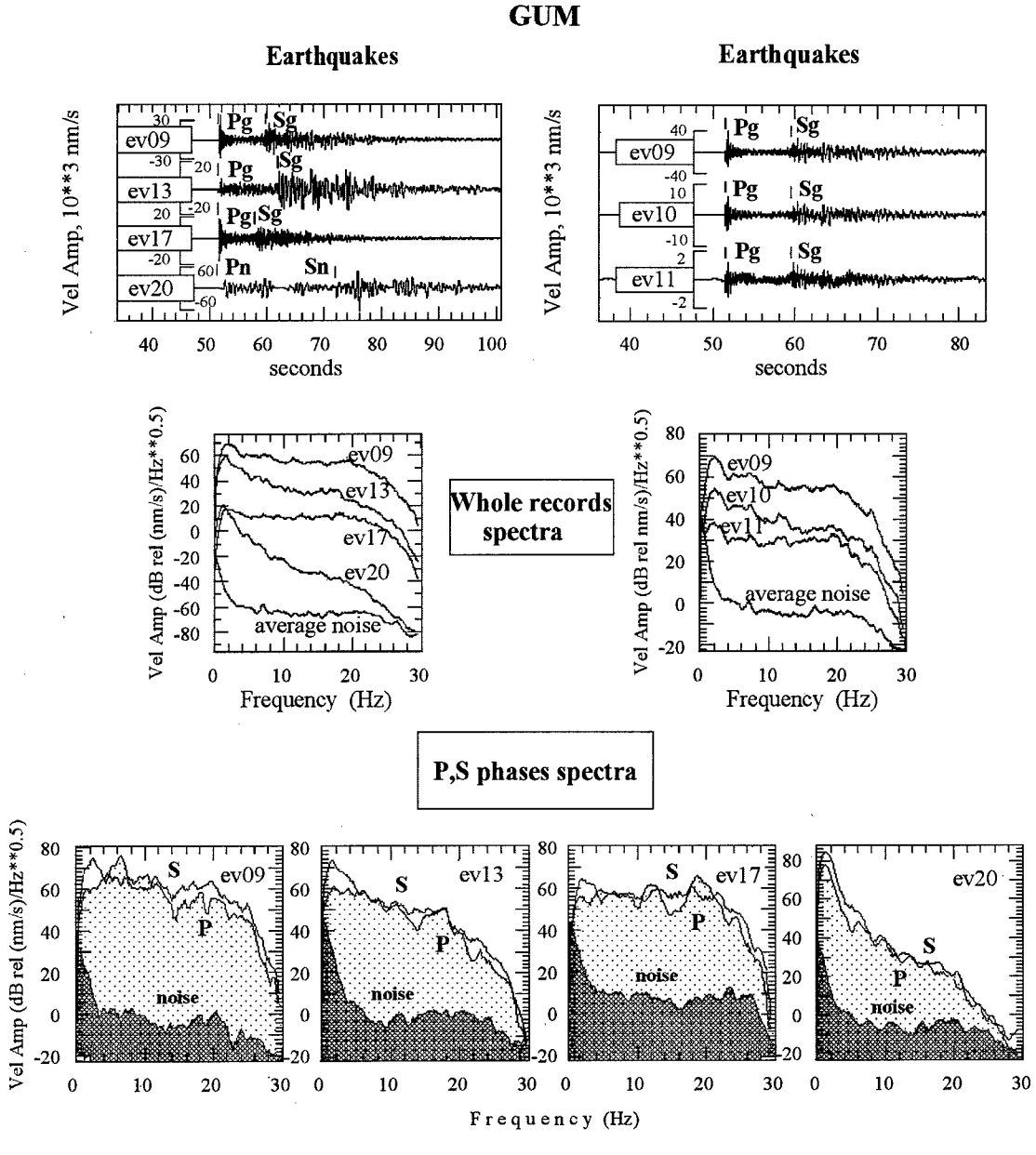

***Fig. 5.4** a - Comparison of Z-component records of regional earthquakes at GUM station (Table 5.1, events 9, 13, 17, 20 - left frame, and events 9, 10, 11 - right frame); b - corresponding whole records spectra For display purposes Z-component spectra of events 13, 17, 20 and average noise are shifted relative upper trace by correspondingly 12, 40, 60, 60 dB; c - P and S phase spectra.*

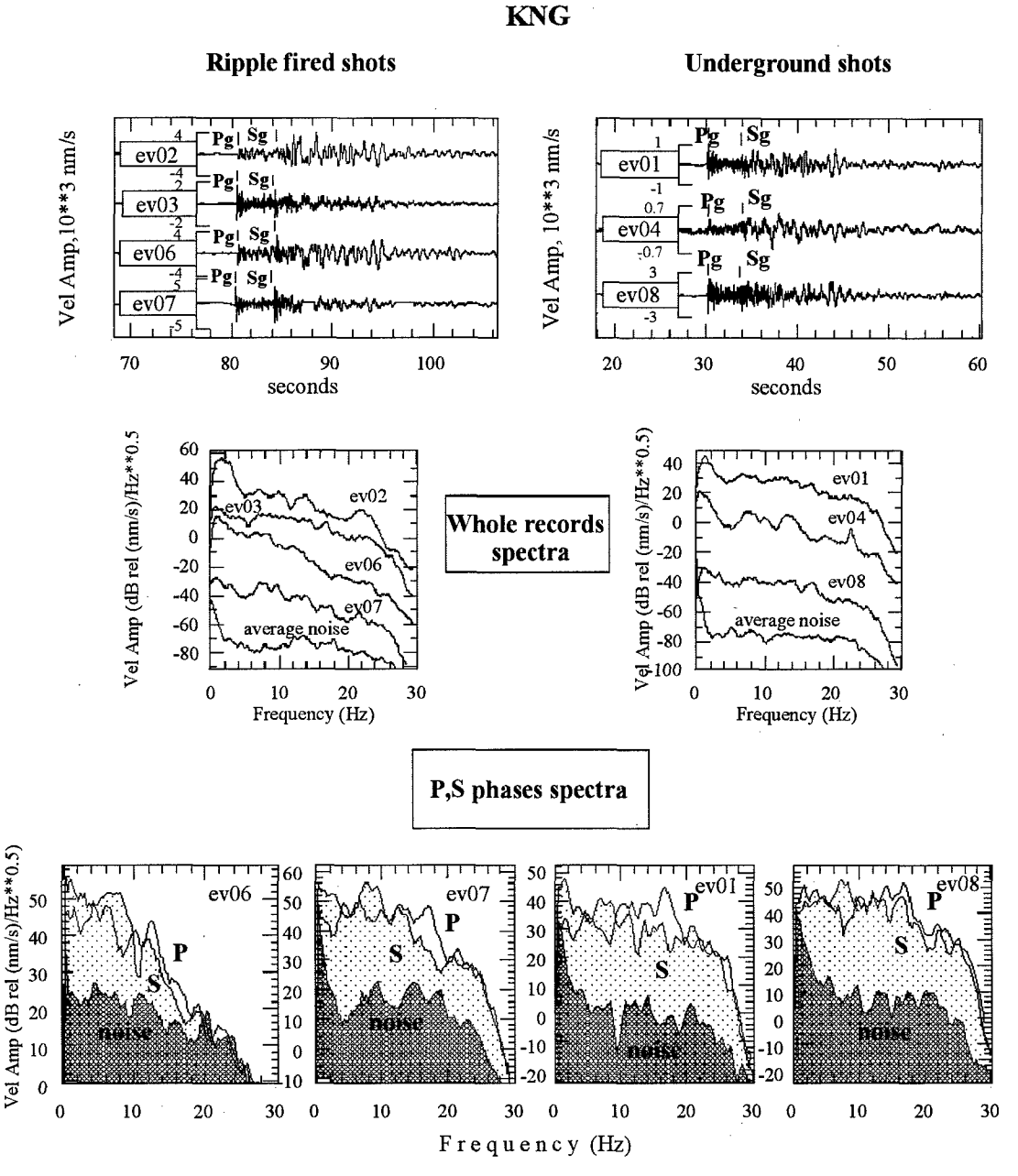

***Fig. 5.5** a - Comparison of Z-component records of ripple fired (l) and underground (g) shots at regional station KNG (Table 5.1, events 1-4,6-8); b - corresponding whole records spectra. For display purposes Z-component spectra are shifted relative upper trace by correspondingly 20, 40, 80, 80 dB (left frame) and 20, 80, 80 dB (right frame); c - P and S phase spectra.*

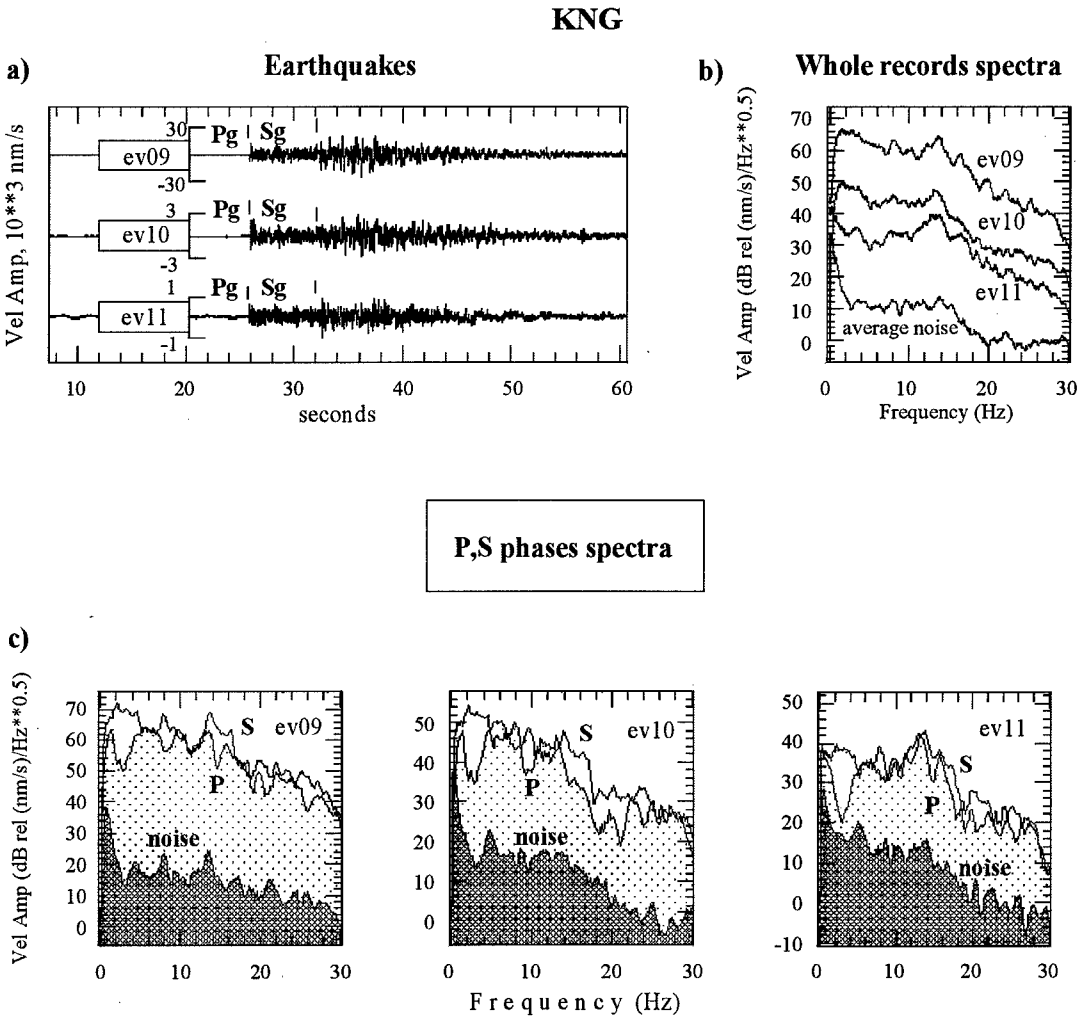

Fig.5.6 a - Comparison of Z-component records of regional earthquakes at KNG station (Table 5.1, events 9, 10, 11); b - corresponding whole records spectra), c - P and S phases spectra.

the segment containing all first arrival P waves being used for spectral estimate calculation. Likewise *S phase* is used to denote the segment containing all S waves arrivals. In the same way, figures 5.2, 5.4, 5.6 represent earthquakes records with whole records and P, S phase spectra. For KIV and GUM stations 2 sets of earthquakes records are plotted: upper left - events 9, 13, 17, 20 located at different seismic zones of the region, upper right - events 9 - 11 from the same zone and close origin times (these events occured in about the same place in 15 minutes time interval). KNG station was taken out of operation in the beginning of 1994 and was reinstalled only to record quarry blasts during the experiment. For this station Fig. 5.6 represents earthquakes 9 - 11 records only with whole records and P, S phases spectra. The strait lines on KNG (event 7) and GUM (event 20) records are caused by data loss in radio channel.

The waveforms from underground and ripple fired shots records look significantly different at KIV and GUM stations, that have similar epicentral distances and 36 degrees azimuth difference. Waveforms features depend on both sourse and travel path

influence. KIV(Z) records have emergent, low frequency first arrival espacially from underground shots (Figure 5.7). Strong negative onset is observed in 100 - 150 ms after first arrival that can easily lead the interpretator into error when undergroung shot with small signal/noise ratio is processed. Similar strong negative onset from underground shot (event 8 from Table 5.1) was observed at local stations BH and LB. This strong negative onset following the first arrival may be caused by the wave, reflected close to shooting area. Relatively low frequency Pg onsets on both KIV and GUM stations can be explained by the presence of big worked out cavities below the source, that act as lowpass filter.

There are strong Pb wave arrival on KIV records in 1.9 s after Pg onset. This phase has about 3 - 5 times bigger amplitude and higher frequency content in comparison with Pg. Pb is observed at GUM records with amplitude close to one of Pg and higher frequency content also. So, KIV records have strongly suppressed Pg arrival relative to Pb one. According to regional tectonic map there is a fault at about 20 km distance to the south from KIV. It spreads close to perpendicular to the line connecting source and KIV station. This fault seems to be an obstacle for Pg wave beam when Pb wave beam spread below it.

Comparison of both whole records and P, S phases spectra (Fig. 5.1, 5.3, 5.5; b, c) shows that for each station underground explosions spectra have enriched high frequency content relative to ones of ripple fired shots. Similar to near-source records spectra (Fig. 3.7) the Oct, 16 ripple fired shot has poor high frequency content in comparison with Nov, 26 one because of different rock in the shooting area.

For each particular record the P and S phase spectra have similar modulation at KIV and GUM stations for both ripple fired shots, events 6 - 7, and separated in space underground, event 8, one (Figures 5.1, 5.3). This similarity is not so noticeable for KNG records. As it was observed earlier by many authors (e.g., Baumgardt and Ziegler, 1988) the spectra of earthquakes have no brightly expressed modulation.

When analyzing multiple-hole instantaneous quarry blasts and ones with 9- or 18-ms delay times Kim *at al.*, 1994 have found the lack of coherent spectral peaks for seismograms from these events recorded at different stations comparing to ripple fired events with total duration 300 -700 ms. Figures 5.1, 5.3, 5.5; b, c also demonstrate the lack of coherent spectral peaks at KIV, GUM, KNG stations for events with 40 - 60 ms total duration. The lack of coherent spectral peaks at these stations was also observed for 1993 experiment data (Stump *et al.*, 1994) for events with 120 and 200 ms total duration. The observations at near-source and local distances let us assume that the lack of coherent spectral peaks at KNG, KIV and GUM stations is probably caused by appearance of echo-signals generated close to the shooting area. These echo-signals interfere with shooting pattern delays. As far as delay depends on source - *reflecting surface* - station relative positions these signals, being observed at different stations with different delays, tend to appearance of noncoherent but stable in time frequency domain spectral maxima and minima. For KIV station the mimimum at 16 Hz on Oct, 16 ripple fired shot spectrogram (Fig. 5.8) lasts about during 20 seconds after onset. Both P and S phase spectra of Nov, 27 underground shot record have minimum at 11 Hz. P wave spectrum has also minimum at 16 Hz. Corresponding minimum in S phase spectrum is broader. The spectrogram of this event record (Fig. 5.8) confirms that 11 Hz minimum lasts about 20 second after onset and one at 16 Hz rapidly comes to noise level. The spectrogram of Nov, 26 ripple fired shot recorded at GUM station has rather stable minima at 7 and 11-12 Hz.

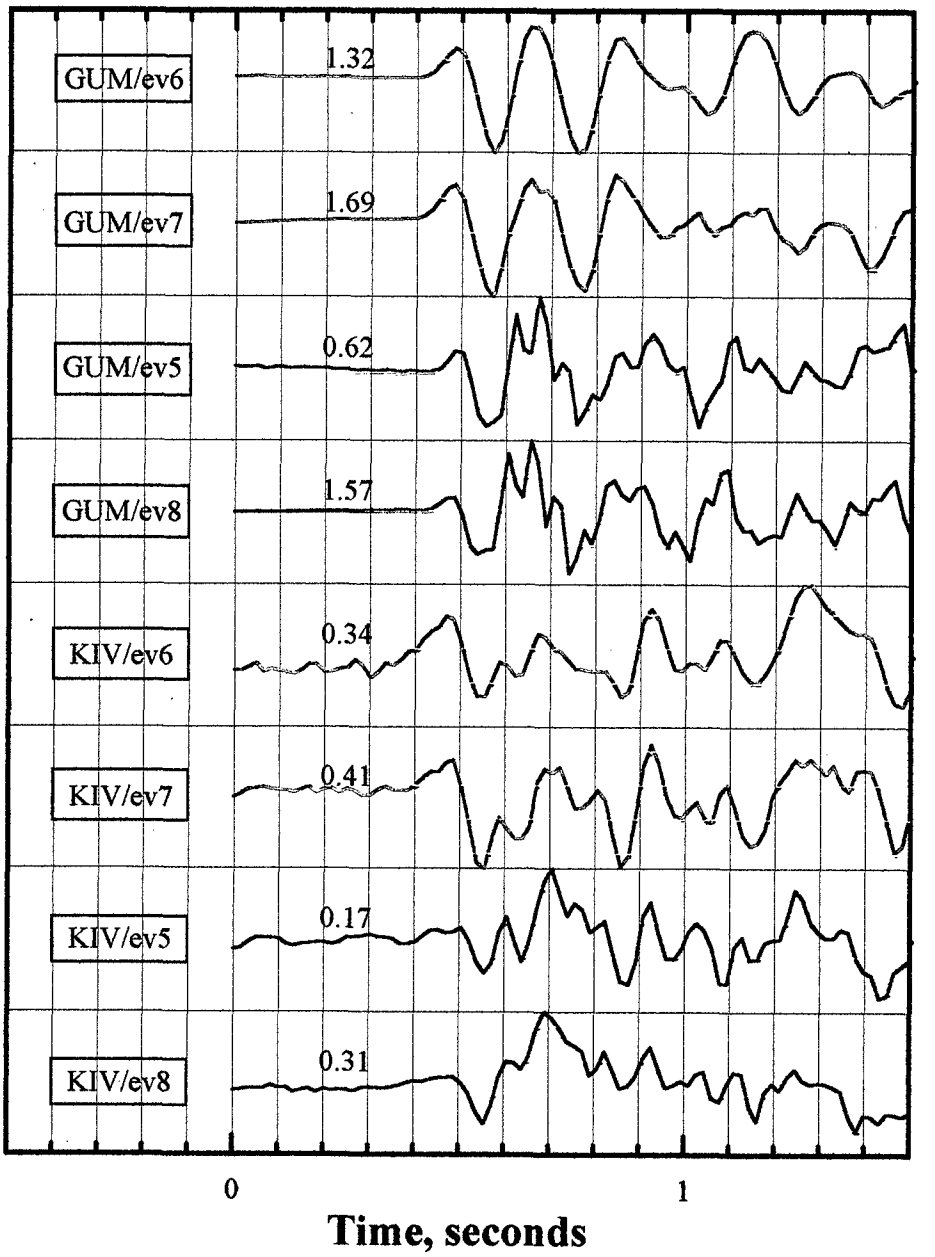

Fig.5.7 Z - component normalized records of onsets from ripple fired (events 6 and 7 from Table 5.1) and underground (events 5 and 8) shots recorded at GUM and KIV stations. The coefficients of normalization are shown in the beginning of each trace and are equal to the maximum velocity amplitude (micron per second) of particular record.

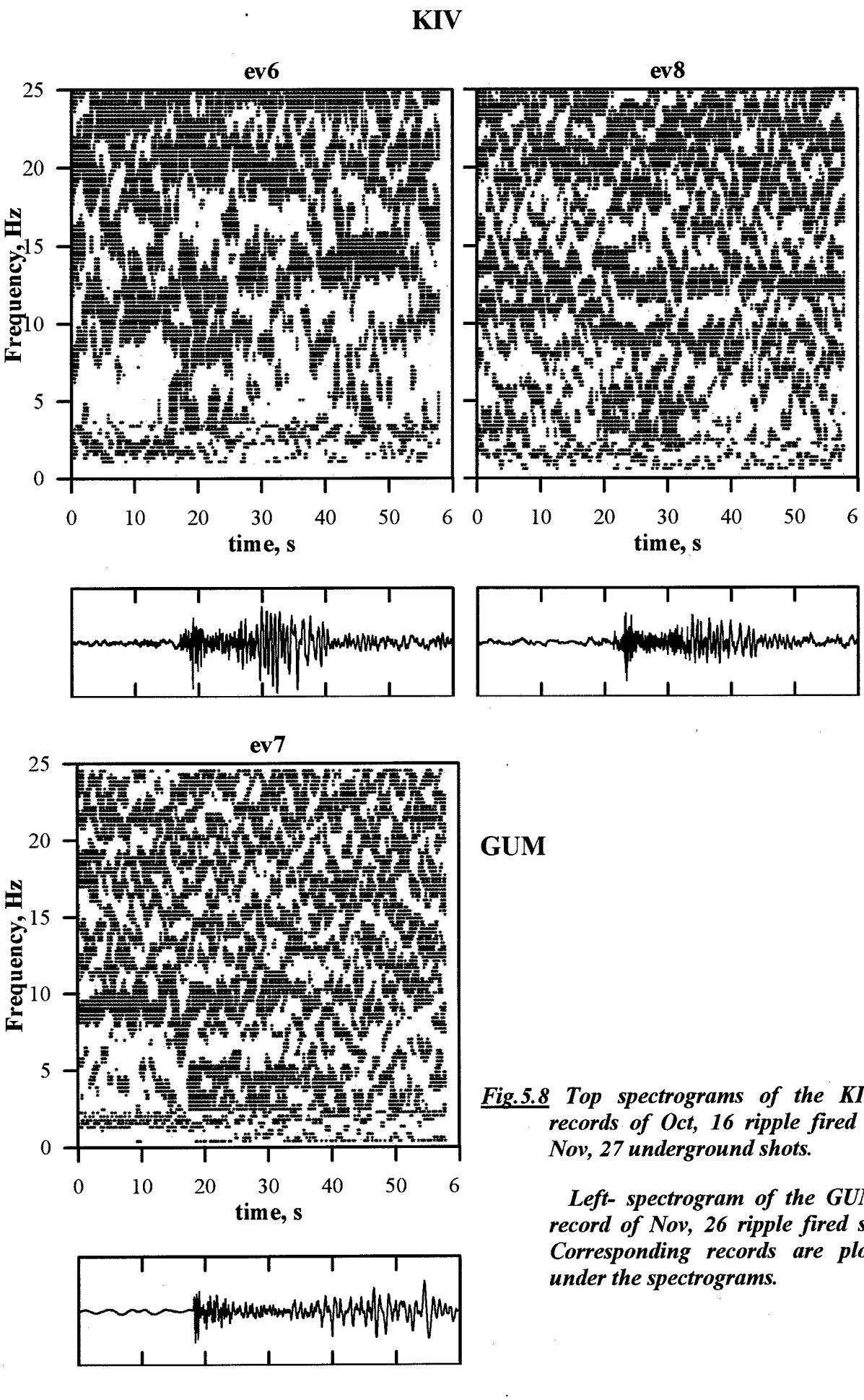

Fig.5.8 ***Top spectrograms of the KIV(z) records of Oct, 16 ripple fired and Nov, 27 underground shots.***

Left- spectrogram of the GUM(z) record of Nov, 26 ripple fired shot. Corresponding records are plotted under the spectrograms.

Demeaned segments of 60 seconds length were selected to calculate spectrograms of KIV and GUM stations records. The segments include about 20 seconds of pre-event noise record. Spectral estimates were calculated for 2 seconds of data in running window using cosine tapering and 250 ms step (overlapping). To get spectrogram each spectral estimate was convolved with different boxcar functions to resolve time-independent spectral modulation. Boxcar functions spanning 10 and 2 Hz were used for spectral estimates smoothing.

P/S spectral amplitude ratios were estimated at frequencies higher than 10 Hz for the data obtained during the experiments in 1993 and 1994 and regional earthquakes from Table 5.1. These ratios were found varying for KIV and GUM stations with mean value 2.4 ± .4 for KIV and 2.2 ± .6 for GUM, having also no meaningful difference for ripple fired and underground shots. For KNG station it varies from 1.0 to 2.1 with mean value of about 1.8. Similar values for 10 regional earthquakes equal to 0.8 - 1.0 and decrease to 0.5 - 0.6 for two most distant events 19 - 20 (Table 5.1). So, for both instantaneous underground (single and separated in space) and ripple fired shots with total duration 40 - 200 ms P/S spectral amplitude ratios are similar to ones, obtained by Kim *et al.*, (1994), for shots with total duration up to 18 ms.

Cluster analysis of waveforms

Despite of the fact that each station displays for quarry blasts and earthquakes records certain differences both in time and in frequency domain, well tested spectrogram method and cepstral analysis are of restricted use being applied to the records with 20-40ms delays. Riviere-Barbier and Grant (1993) have applied a method of the hierarchical claster analysis to identify and locate closely spaced mining events. They used maximum value of cross-correlation function between envelopes of the whole signal records as a measure of similarity between pairs of events. This numbers constitute the elements of a matrix used in the claster analysis in complete linkage method.

Application of clustering algorithms to a set of waveforms together with appropriate displays of the clustering results is very useful for justification of possibility of classification: if well-clustered group of waveforms with similar sources or propagation paths is observed then a high-quality classifier correlated with this clustering can be implemented.

Let $W = \{w_1, \ldots, w_N\}$ be a set of waveforms. For any two waveforms $w_i, w_k \in W$ a distance (dissimilarity) $d(w_i, w_k) \geq 0$ may be introduced (Jambu, 1978). over the maximum crosscorrelation of their envelopes $-1 \leq r(w_i, w_k) \leq 1$ with monotonous transform:

$$d(w_i, w_k) = \frac{1 - r^2(w_i, w_k)}{r^2(w_i, w_k)}.$$

By a *partition* of W we understand a system $P = (P_1, \ldots, P_K)$ of disjoint subsets-*clusters* $P_i \subseteq W$ with $W = \bigcap_{i=1}^{K} P_i$ and $P_i \cap P_k = \varnothing$ for any $1 \leq i, k \leq K$. A *hierarchy*

of W is a system of partitions $P_0,\ldots,P_M$ with $P_0 = \left(\{w_1\},\ldots,\{w_N\}\right)$, $P_M = W$, and P_i is a refinement of P_j for all $0 \le i < j \le M$.

Here agglomerative hierarchical pair-group clustering methods are considered. Starting with a set of N waveforms to be clustered, they group themselves into successively fewer than N sets arriving at a single set W containing all waveforms. At each iteration exactly two clusters (whose distance is minimal) are agglomerated into a single cluster. The same algorithm is used iteratively to generate P_{i+1} from P_i for all $0 \le i < M$. A unified efficient algorithm exists (Jambu, 1978) to compute the new distances after every iteration.

The minimal distance between the agglomerated clusters serves as a monotonous index of the partitions hierarchy $h(P_i)$, with $h(P_0) = 0$. Such an indexed hierarchy may be represented by a *dendrogram*.

The clustering methods are distinguished on the basis of the distance measure used between clusters. In the *single linkage* method the minimal distance between the elements of the clusters P_i and P_k is taken:

$$D_S(P_i, P_k) = \min_{\substack{w_l \in P_i \\ w_m \in P_k}} d(w_l, w_m).$$

In this method a cluster is defined as a set of points all of which are within some critical distance of at least one other member of the cluster. The method uncovers those groups that appear to be intertwined lines in multidimensional space, but in many cases this leads to chaining effect making the clusters meaningless.

In the *complete linkage* method the distance measure between P_i and P_k is defined as the maximal distance of their elements:

$$D_C(P_i, P_k) = \max_{\substack{w_l \in P_i \\ w_m \in P_k}} d(w_l, w_m).$$

Here a cluster is defined as a set of points all of which are within some critical distance. In opposition to the single linkage this method generates very homogeneous clusters.

In the *average linkage* method the mean distance between the objects of both classes is selected as the distance between the clusters P_i and P_k :

$$D_A(P_i, P_k) = \frac{1}{|P_i| \cdot |P_k|} \sum_{\substack{w_l \in P_i \\ w_m \in P}} d(w_l, w_m).$$

The average linkage method stands between single and complete linkage and thereby profits from the stability of the one and the homogeneous property of the other method.

Three clustering methods -- *single linkage, complete linkage* and *average linkage* -- were applied here to 20 Z-component records at KIV station listed in Table 5.1: 4 ripple fired and 4 underground shots, documented during experiments of 1993 (Stump et al., 1994) and 1994, and 12 earthquakes of several zones of a region (Table 2). Due to discrepancy between official mine records and actual blasting practice it is hard to involve other shots records into analysis. Cross-correlation functions between envelopes of all records (30s, including 3s before onset) for each pair of events were calculated.

The dendrogram for these tree methods are shown in figures 5-9 - 5.11. Here the numbers in the left side of the tree correspond to events numbers from Table 5.1. Coordinates of vertical lines correspond to the distance between events and/or clusters. The values of these distances are printed close to appropriate vertical line.

The results obtained by *single linkage* method are unsatisfactory. For distance D = 3 earthquakes 16 - 18 and 19 - 20 are included into the common group with 6 quarry blasts when 2 explosions (4 and 7) fell out of this group.

Complete linkage and *average linkage* methods give successful and very similar results. All quarry blasts are allocated in common group, containing none of 12 chosen earthquakes. The records of earthquakes have formed 4 groups according to their epicentral distances.

It is remarkable that in dendrogram obtained by *complete linkage* method the quarry blasts records are divided in 2 subgroups. One includes events, consisting from 1 or 2 shots separated in space or in time, and other - events, consisting from 3-7 shots. The only exception is event 5, whose waveform according to near-source data analysis contains multiple echo- signals. The fact of this blasts waveform separation prompts that the method may be sensitive not only to events location but also to their "simplicity" and can be useful for discrimination purposes.

Classification of waveforms

It has been shown that seismic waveforms of regional earthquakes and Tyrnyauz mine explosions recorded at KIV station form separate clusters in the hierarchy given by complete linkage and average linkage clustering algorithms. Here a simple classification method is presented to discriminate these two classes of waveforms.

We generalize a quantitative specification of pairwise dissimilarity based on the maximum crosscorrelation of envelopes $d(w_i, w_k)$ to the dissimilarity $d(w, C)$ between a single waveform w and a class of waveforms C by the formula:

$$d(w, C) = \min_{\{w_i\} \in C} d(w, w_i).$$

Let the two classes of waveforms C_1 and C_2 be given. The union $C_1 \cup C_2$ is called learning set. To classify a waveform w from a test set we use the *nearest neighbour* decision rule:

$$w \in \begin{matrix} C_1 \\ C_2 \end{matrix}, \text{ if } d(w, C_1) \begin{matrix} \leq \\ > \end{matrix} d(w, C_2)$$

An error rating of the classification comes from a *cross validation* method (Hand, 1986). One by one we omit a waveform from the learning set and test it using the remaining learning data. The error rating is the percentage of misclassifications across all omitted waveforms. For seismic records in Table 5.1 the error rate of the nearest neighbour classification between earthquakes and explosions is 20%: earthquakes 12, 15, 19, 20 are misclassified as explosions.

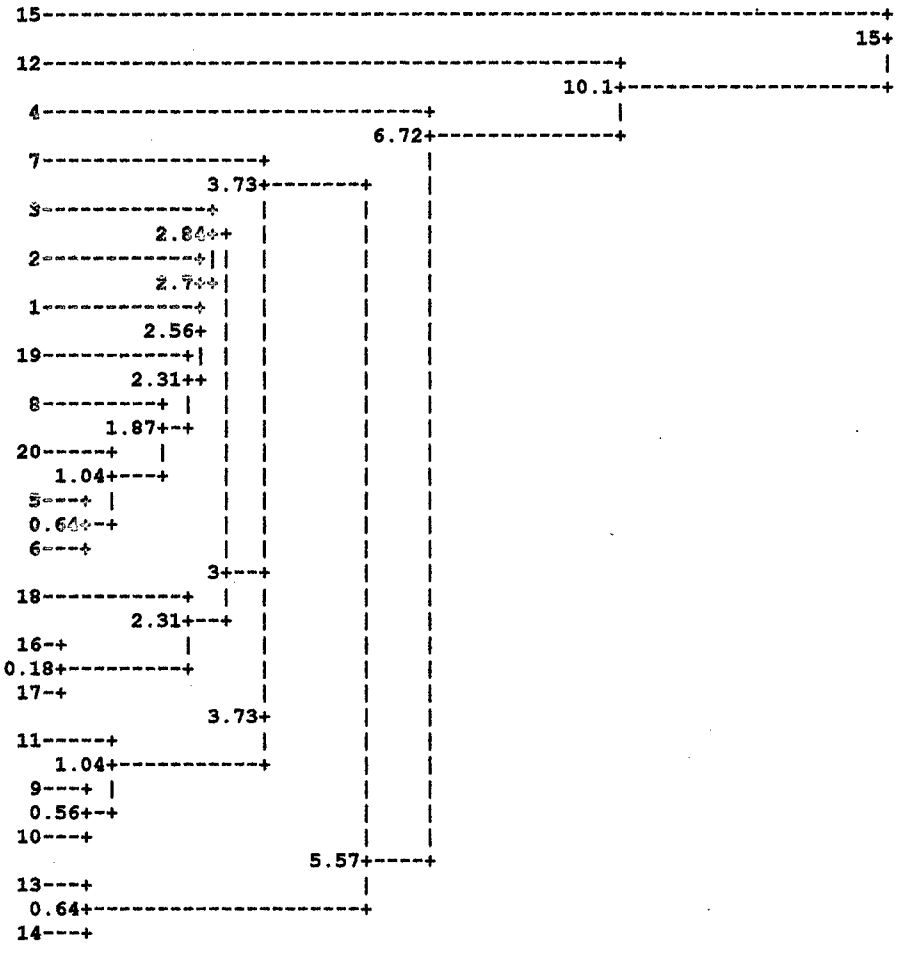

***Fig. 5.9** Single linkage dendrogram for KIV(z) records (Table 5.1, events 1-20). Coordinates of vertical lines correspond to the distance between events and/or clusters. The value of particular distance is printed close to appropriate vertical line.*

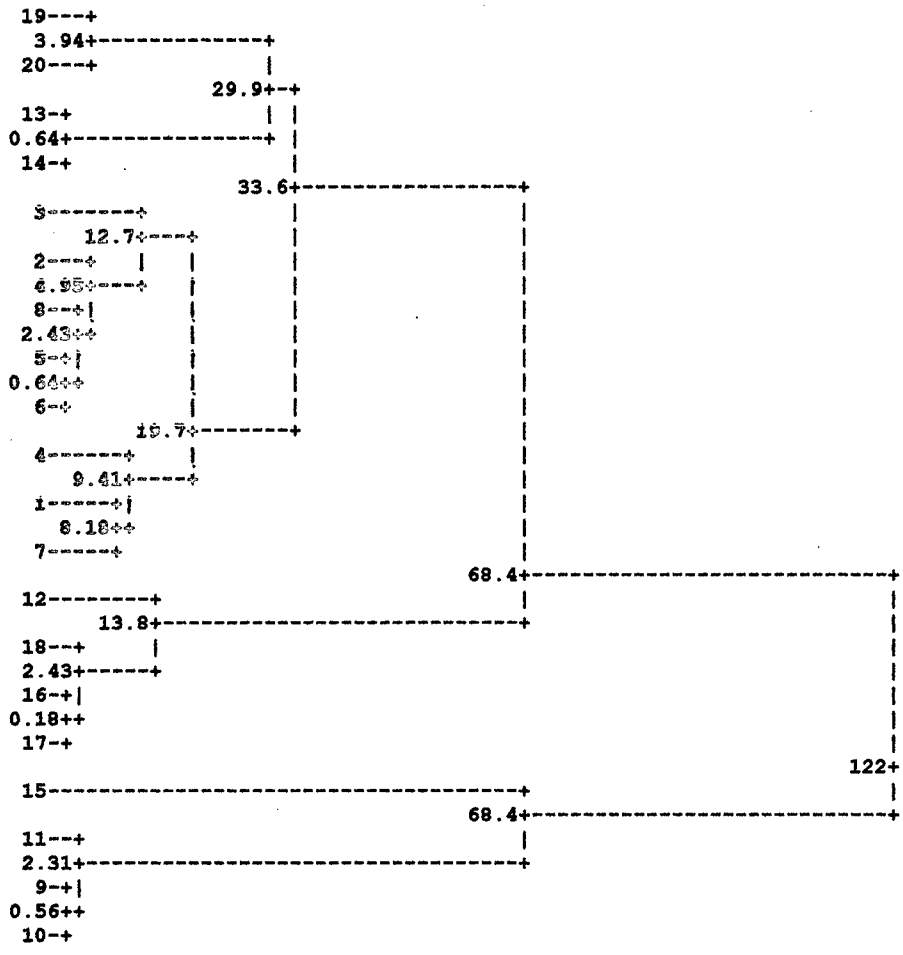

***Fig. 5.10** Complete linkage dendrogram for KIV(z) records (Table 5.1, events 1-20). Coordinates of vertical lines correspond to the distance between events and/or clusters. The value of particular distance is printed close to appropriate vertical line.*

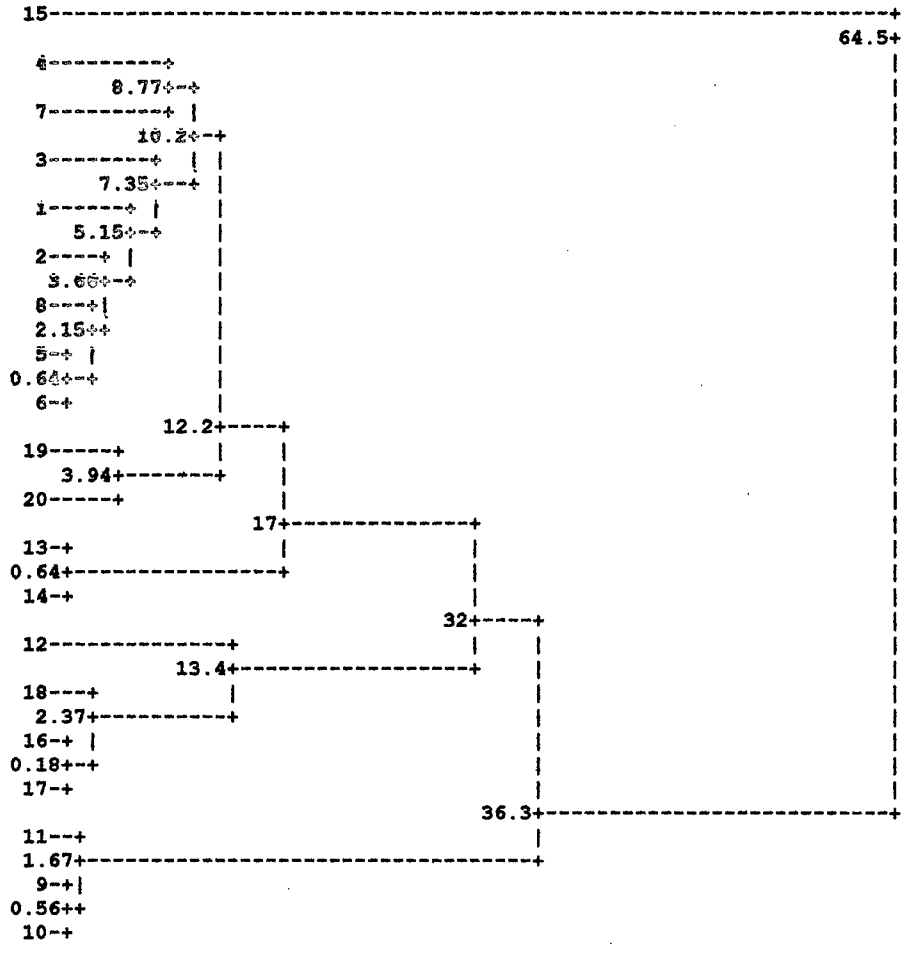

Fig.5.11 *Average linkage dendrogram for KIV(z) records (Table 5.1, events 1-20). Coordinates of vertical lines correspond to the distance between events and/or clusters. The value of particular distance is printed close to appropriate vertical line.*

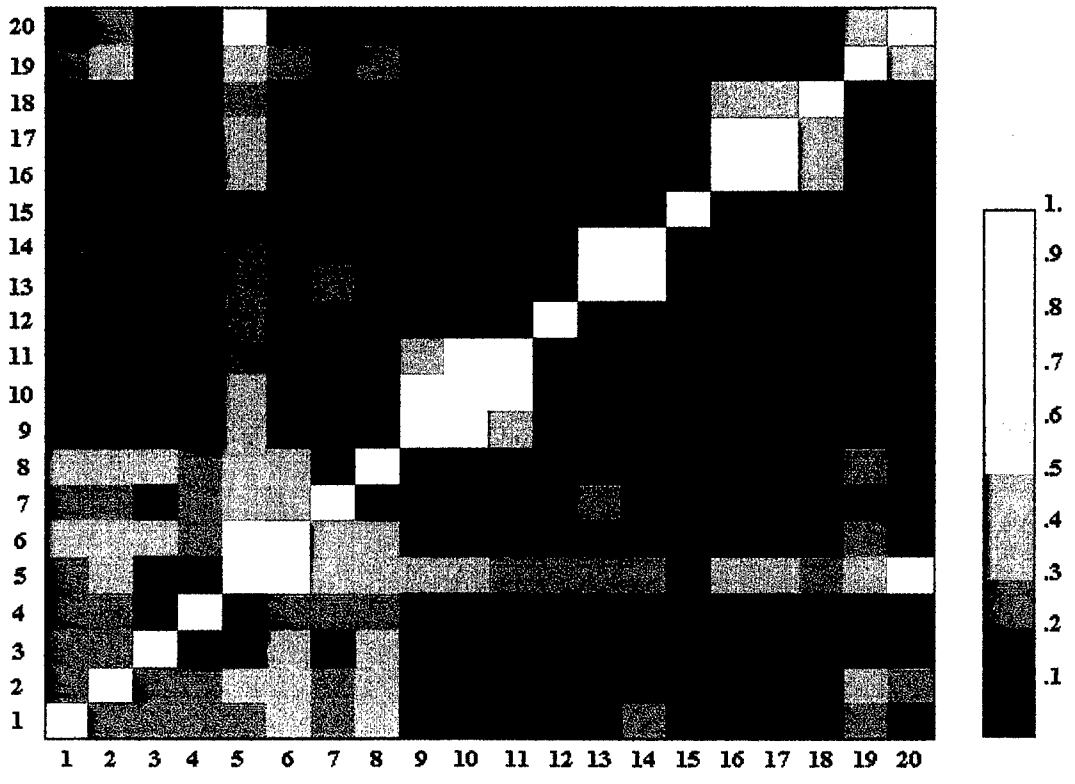

***Fig. 5.12** Crosscorrelation matrix for 20 events from Table 5.1. Right -- the color palette representing corresponding crosscorrelation values.*

The "jack knife" method was used to refine learning set and estimate the classification stability. Every waveform is temporarily removed from the learning and the cross validation error rate is computed for all such cases. Classification of data set in Table 5.1 appears stable until the explosion waveform 5 is removed from learning: in this case the only earthquake 15 is misclassified which is poorly determined *a priori*. Such a particular behavior of well documented underground event 5 (Table 5.1) can be explained by the fact of rather high correlation between its waveform envelope and earthquakes ones due to the local structures influence in the source area. This correlation is prominently expressed by crosscorrelation matrix for events from the Table 5.1 (Fig. 5.12). Here crosscorrelation values are represented with different colors. Both explosions and earthquakes are grouped in clusters similar to represented in dendrogram in figures 5.10 and 5.11, and event 5 has significant crosscorrelation value with most of earthquakes.

6. Conclusions.

The experiment has been conducted in October - November 1994 in southern Russia at Tyrnyauz mine in the Caucasus Mountains. Due to sophisticated topography and ore lode location, production shots in this mine are carrying out both near surface and 200-700 meters below it in the same vertical plane between 2000 and 3000 m above see level. During this experiment waveforms generated by well documented close located single (210 and 420 kg), ripple fired near-surface shots (11.97 and 8.19 tons) and underground (9.3 and 24.5 tons) ones have been recorded at near-source (200 - 400 m from near-surface shots) distances. Ripple fired and underground shots were also recorded at local (1.5 - 5 km) and regional (25 - 70 km) distances.

Near-source data analysis has shown that in Tyrnyauz mine the shift of the source on a few tens of meters effects strongly on wave propagation conditions. Synthetic seismograms were obtained by convolving single shot record with a set of impulses whose time positions include delays for both inter row detonations and traveltimes. The amplitudes of synthetic records of Oct, 16 ripple fired shot are significantly bigger in comparison to real one. It seems to be caused mainly by poor representation of week and shallow subshots by 2-5 times stronger calibration one: the hole of Oct, 17 single shot (10 m deep) crossed stripping rock layer and became buried in competent rock. Both topography and big underground cavities between source and station result in generation of echo-signals that distort delays pattern expected from Nov, 26 short design. Comparison of synthetic and ripple fired shot records shows that here the envelope similarity was achieved on the intervals up to 0.3 - 0.5s after onset only (about up to 20% of the records duration).

Both Nov, 26 ripple fired near-surface shot and separated in space Nov, 27 underground one have produced spectral modulation of records obtained at local distances (1.6 - 5.6 km). For all stations the spectrograms of ripple fired shot have minimum whose position corresponds to the only minimum of the modulation function in the instrument passband (0.4 - 20 Hz). Three subshots of underground explosions occurred 150 - 250m from each other. For shots separated by such distances delays between signals from different subshots will be close to delays between rows detonation for Nov, 26 ripple fired shot and can cause the observed spectral modulation. Both particular form of onsets and spectral modulation suggest that seismograms recorded at PW, BH and LB stations contain echo-signal generated close to shooting area.

Data obtained during experiments in 1993 (Stump *et al.*, 1994) and 1994 were compared with seismograms of 12 regional earthquakes recorded at regional stations GUM, KIV and KNG. Spectral and cluster analysis of the waveforms was implemented to discriminate between mine blasts and regional earthquakes records.

Comparison of both whole records and P, S phases spectra shows that for each station underground explosions spectra have enriched high frequency content relative to ones of ripple fired shots. Similar to near-source records spectra the Oct, 16 ripple fired shot has poor high frequency content in comparison with Nov, 26 one because of different rock in the shooting area.

P/S spectral amplitude ratios were estimated at frequencies higher than 10 Hz for the data obtained during the experiments in 1993 and 1994 and regional earthquakes. For

both instantaneous underground (single and separated in space) and ripple fired shots with total duration 40 - 200 ms P/S spectral amplitude ratios are similar to ones, obtained by Kim *et al.*, (1994), for shots with total duration up to 18 ms. These ratios were found varying for KIV and GUM stations with mean value 2.4 ± .4 for KIV and 2.2 ± .6 for GUM, having also no meaningful difference for ripple fired and underground shots. For KNG station it varies from 1.0 to 2.1 with mean value of about 1.8. Similar values for 10 regional earthquakes equal to 0.8 - 1.0 and decrease to 0.5 - 0.6 for two most distant events 19 - 20 (Table 5.1).

Three clustering methods -- *single linkage, complete linkage* and *average linkage* -- were applied to 20 Z-component records at KIV station: 8 well documented Tyrnyauz mine blasts and 12 earthquakes of several zones of a region .*Complete linkage* and *average linkage* methods give successful and very similar results. All quarry blasts are allocated in common group, containing none of 12 chosen earthquakes. The records of earthquakes have formed 4 groups according to their epicentral distances.

One nearest neighbour classification rule was successfully applied to discriminate quarry blasts and small earthquakes records at distances 20 - 200 km. The complete linkage dendrogram structure promises to be useful in visualization of the simple and multiplicative shots classification process when sufficient amount of learning data are available.

Acknowledgments

The authors are grateful to many people in Institute of Physics of the Earth for fruitful discussions. Special thanks go to G. Kagan, the operator of Tyrnyauz mine, and EME staff: Yu. Zhukov and O. Isay for assistance in the field observation, V. Babkina and A. Akimov - in data processing, S. Krasilov - for image processing.

References

Baumgardt, D.R. and K.A.Ziegler (1988). Spectral evidence for source multiplicity in explosions: application to regional discrimination of earthquakes and explosions. Bull.Seism.Soc.Am. 78, 5, 1773-1795.

Hand, D.J (1986) Recent advances in error rate estimation. Pattern Recognition Letters, 4, 1986, p. 335-346.

Hedlin, M.A.H., J.B.Minster, and J.A.Orcutt (1989). The time-frequency characteristics of quarry blasts and calibration explosions recorded in Kazakhstan, USSR, Geophys. J. 99, 109-121.

Hedlin, M.A.H., J.B.Minster, and J.A.Orcutt (1990). An Automatic means to discriminate between earthquakes and quarry blasts. Bull.Seism.Soc.Am. 80, 6b, 2143-2160.

Jambu, M. (1978). Classification automatique pur l'analyse des donnees. 1 - Metodes et algorithmes. DUNOD, Paris, 310pp.

Kim, W.Y., D.W.Simpson, and P.G.Richards (1994). High-FrequencySpectra of Regional Phases from Earthquakes and Chemical Explosions. Bull.Seism.Soc.Am. 84, 5, 1365-1386.

Markel, J.D and Gray, A.H., 1976. Linear Prediction of Speech, Springer-Verlag, Berlin, Heidelberg, New York.

Nicholls, H.R., C.F. Johnson, and W.I. Duvall (1971). Blasting vibrations and their effects on structures, Bureau Mines Bull. 656, U.S. Dept. of the Interior, Washington, D.C., 105pp.

Reamer S.K., K.-G. Hinzen and B.W. Stump (1992) Near-source characterization of the seismic wavefield radiated from quarry blasts.Geophys.J.Int. 110, 435-450.

Riviere-Barbier,F. and L.T.Grant (1993). Identification and location of closely spaced mining events. Bull.Seism.Soc.Am. 83, 5, 1527-1546.

Stump, B.W. and R.E. Reinke (1988) Experimental confirmation of superposition from small-scale explosions, Bull. Seism.Soc.Am. 78, 1059-1073.

Stump, B.W.,F.Riviere-Barbier, I.Chernobye and K.Koch (1994). Monitoring a Test Ban Treaty presents scientific challenges. Eos Trans. AGU, 75, 24.